EFFECTS OF INTERMEDIATE PRINCIPAL STRESS ON

COMPRESSIVE STRENGTH AND ELASTICITY OF

PHRA WIHAN SANDSTONE

Thanawat Pobwandee

A Thesis Submitted in Partial Fulfillment of the Requirements for the

Degree of Master of Engineering in Geotechnology

Suranaree University of Technology

Academic Year 2010

ผลกระทบของความเค้นหลักกลางต่อกำลังกดและ
ความยืดหยุ่นของหินทรายชุดพระวิหาร

นายธนวัฒน์ พบวันดี

EFFECTS OF INTERMEDIATE PRINCIPAL STRESS ON

COMPRESSIVE STRENGTH AND ELASTICITY

OF PHRA WIHAN SANDSTONE

Suranaree University of Technology has approved this thesis submitted in partial fulfillment of the requirements for the Master's degree.

Thesis Examining Committee

_____

(Asst. Prof. Thara Lekuthai)

Chairperson

_____

(Assoc. Prof. Dr. Kittitep Fuenkajorn)

Member (Thesis Advisor)

_____

(Dr. Prachya Tepnarong)

Member

_____   _____

(Prof. Dr. Sukit Limpijumnong)   (Assoc. Prof. Dr. Vorapot Khompis)

Vice Rector for Academic Affairs   Dean of Institute of Engineering

ธนวัฒน์ พบวันดี : ผลกระทบของความเค้นหลักกลางต่อกำลังกดและความยืดหยุ่นของ
หินทรายชุดพระวิหาร (EFFECTS OF INTERMEDIATE PRINCIPAL STRESS ON
COMPRESSIVE STRENGTH AND ELASTICITY OF PHRA WIHAN SANDSTONE)
อาจารย์ที่ปรึกษา : รองศาสตราจารย์ ดร.กิตติเทพ เฟื่องขจร, 73 หน้า.

วัตถุประสงค์ของการวิจัยนี้เพื่อหากำลังกดและคุณสมบัติความยืดหยุ่นของหินทรายชุด
พระวิหารที่มีผลกระทบจากความเค้นหลักกลาง กิจกรรมหลักประกอบด้วยการทดสอบเพื่อหา
ความเค้นหลักสูงสุดที่จุดวิบัติของหินภายใต้ความเค้นหลักกลางและค่าความเค้นหลักต่ำสุดในหลาย
ระดับและการพัฒนาความสัมพันธ์ทางคณิตศาสตร์ของความเค้นในสามแกนที่จุดวิบัติ
เครื่องกดทดสอบในสามแกนจริงให้ค่าความเค้นหลักกลางและค่าความเค้นหลักต่ำสุดคงที่
ต่อตัวอย่างหินและทำการเพิ่มค่าความเค้นหลักสูงสุดจนถึงจุดวิบัติ   ค่าความเค้นหลักกลางและ
ค่าความเค้นหลักต่ำสุดผันแปรจาก 0   ถึง 60   เมกะปาสคาล ตัวอย่างหินคือหินทรายชุดพระวิหาร
ถูกจัดเตรียมให้มีขนาด 5×5×5 ลูกบาก์ศเซนติเมตร มีการทดสอบอย่างน้อย 40 ตัวอย่าง ซึ่งขึ้นอยู่กับ
ความสอดคล้องของผลการทดสอบหาค่าความแข็งและค่าความยืดหยุ่นของหิน เกณฑ์การแตก
ในสามทิศทางของ Weibols and Cook ได้นำเสนอในรูปของค่าความเค้นเฉือนในสามมิติต่อค่า
ความเค้นเฉลี่ย เกณฑ์ที่ได้สามารถนำไปใช้ในการกำหนดหรือทำนายความแข็งของหินทรายภายใต้
สภาวะความเค้นที่แตกต่างกันในแต่ละทิศทางที่อยู่ในภาคสนามได้

สาขาวิชา<u>เทคโนโลยีธรณี</u>   ลายมือชื่อนักศึกษา _____
ปีการศึกษา 2553   ลายมือชื่ออาจารย์ที่ปรึกษา _____

THANAWAT POBWANDEE : EFFECTS OF INTERMEDIATE PRINCIPAL STRESS ON COMPRESSIVE STRENGTH AND ELASTICITY OF PHRA WIHAN SANDSTONE. THESIS ADVISOR : ASSOC. PROF. KITTITEP FUENKAJORN, Ph.D., P.E., 73 PP.

TRUE TRIAXIAL/INTERMEDIATE PRINCIPAL STRESS/SANDSTONE/ ELASTICITY

The objectives of this research are to determine the compressive strengths and elastic properties of Phra Wihan sandstone as affected by the intermediate principal stress. The efforts involve determination of the maximum principal stress at failure of the sandstone samples under various intermediate and minimum principal stresses, and development of a mathematical relationship between the three principal stresses at failure. A polyaxial loading frame is used to apply constant σ_2 and σ_3 onto the specimen while σ_1 is increased until failure. The applied σ_2 and σ_3 are varied from 0 to 60 MPa. The Phra Wihan sandstone is prepared to obtain cubical shaped specimens with a nominal size of $5\times5\times5$ cm^3. A minimum of 40 samples have been tested, depending on the consistency of the strength results. The failure stresses are measured and modes of failure are examined. The three-dimensional strength criterion of the modified Wiebols and Cook is proposed by presenting the octahedral shear strength as a function of the octahedral mean stress. The research results are useful for determining or predicting the sandstone strength under anisotropic stress states of the in-situ condition.

School of Geotechnology   Student's Signature_____

Academic Year 2010   Advisor's Signature_____

ACKNOWLEDGMENTS

I would like to express my sincere thanks to Assoc. Prof. Dr. Kittitep Fuenkajorn, thesis advisor, who gave a critical review and constant encouragement throughout the course of this research. Further appreciation is extended to Asst. Prof. Thara Lekuthai, chairman of School of Geotechnology and Dr. Prachya Tepnarong, School of Geotechnology, Suranaree University of Technology who are member of my examination committee. Grateful thanks are given to all staffs of Geomechanics Research Unit, Institute of Engineering who supported my work.

Finally, I most gratefully acknowledge my parents and friends for all their supported throughout the period of this research.

Thanawat Pobwandee

TABLE OF CONTENTS

Page

CHAPTER

TABLE OF CONTENTS (Continued)

TABLE OF CONTENTS (Continued)

Page

LIST OF TABLES

LIST OF FIGURES

Figure   **Page**

LIST OF FIGURES (Continued)

LIST OF SYMBOLS AND ABBREVIATIONS

A	=	Parameter related to C_0 and μ_i
B	=	parameter related to C_0 and μ_i
C	=	Parameter related to C_0 and μ_i
C_0	=	Uniaxial compressive strength
C_1	=	Parameter related to C_0 and μ_i
c	=	Cohesion
E	=	Elastic modulus
J_1	=	The first order of stress invariant
$J_2^{1/2}$	=	The second order of stress invariant
S_o	=	Cohesion
ε_1	=	Axial strain
$\varepsilon_2, \varepsilon_3$	=	Lateral strain
ν	=	Poisson's ratio
σ_m	=	Mean stress
σ_n	=	Normal stress
σ_1	=	Maximum principal stress
σ_2	=	Intermediate principal stress
σ_3	=	Minimum principal stress
τ	=	Shear stress
τ_{oct}	=	Octahedral shear stress
ϕ	=	Friction angle

CHAPTER I

INTRODUCTION

1.1   Background and rationale

It has been experimentally found that the intermediate principal stress (σ_2) can notably reduce the maximum principal stress (σ_1) at failure for intact rock specimens. This suggests that the triaxial compressive strengths obtained from the conventional triaxial compression test (under $\sigma_2 = \sigma_3$), may not truly represent the actual in-situ strength where the rock is subjected to an anisotropic stress state ($\sigma_1 \neq \sigma_2 \neq \sigma_3$). The rock failure criterion derived from such conventional testing therefore may not be conservative. Obtaining rock strengths in the laboratory under an anisotropic stress state is not only difficult but expensive. Special loading device (e.g., polyaxial loading machine or true triaxial load cell) is required. As a result the failure criterion that can take into account the three-dimensional stress states has been extremely rare. The existing three dimensional failure criteria for brittle rocks are not adequate because they are not in the form that can readily be applied in the actual design and analysis of geological structures.

1.2   Research objectives

The objectives of this research are to determine the compressive strengths of Phra Wihan sandstone subjected to anisotropic stress states, and to develop a three-dimensional failure criterion of the rocks that can be readily applied in the design and

stability analysis of geologic structures. The efforts involve determination of the maximum principal stress at failure of the rock samples under various intermediate and minimum principal stresses, and development of a mathematical relationship between the three stresses at failure. A polyaxial loading frame is used to apply constant σ_2 and σ_3 onto the specimen while the σ_1 is increased until failure. The applied σ_2 and σ_3 at different magnitudes are varied from 0 to 60 MPa. The failure stresses are measured and modes of failure are examined. The results compared with those obtained from the conventional triaxial compressive strength tests. The three-dimensional strength criterion is derived by presenting the octahedral shear strength and a function of the octahedral mean stress with correction factors if needed. Such criterion is useful for determining or predicting the rock strength under anisotropic stress states of the in-situ condition.

1.3   Research methodology

The research methodology shown in Figure 1.1 comprises 5 steps; literature review, sample preparation, polyaxial compressive testing, development of mathematical relations and discussions and conclusions.

1.3.1   Literature review

Literature review is carried out to study the previous research on compressive strength in true-triaxial state and effect of intermediate principal stress. The sources of information are from text books, journals, technical reports and conference papers. A summary of the literature review are given in the thesis.

1.3.2   Sample preparation

Sandstone samples are collected from the site. Laboratory experiments are conducted on rock specimens from Phra Wihan formation. Sample preparation is

carried out in the laboratory at the Suranaree University of Technology. Samples prepared for compressive strength test are $5\times5\times5$ cm^3.

```
┌─────────────────────────────────┐
│                                 │
│       ┌───────────────────┐     │
│       │ Literature Review │     │
│       └───────────────────┘     │
│                 │               │
│                 ↓               │
│       ┌───────────────────┐     │
│       │ Sample Preparation│     │
│       └───────────────────┘     │
│                 │               │
│                 ↓               │
│       ┌───────────────────┐     │
│       │ Polyaxial         │     │
│       │ Compression       │     │
│       │ Testing           │     │
│       └───────────────────┘     │
│                 │               │
│                 ↓               │
│       ┌───────────────────┐     │
│       │ Development        │    │
│       │ of Mathematical    │    │
│       │ Relations          │    │
│       └───────────────────┘     │
│                 │               │
│                 ↓               │
│       ┌───────────────────┐     │
│       │ Discussions and    │    │
│       │ Conclusions        │    │
│       └───────────────────┘     │
│                 │               │
│                 ↓               │
│       ┌───────────────────┐     │
│       │ Thesis Writing    │     │
│       └───────────────────┘     │
│                                 │
└─────────────────────────────────┘
```
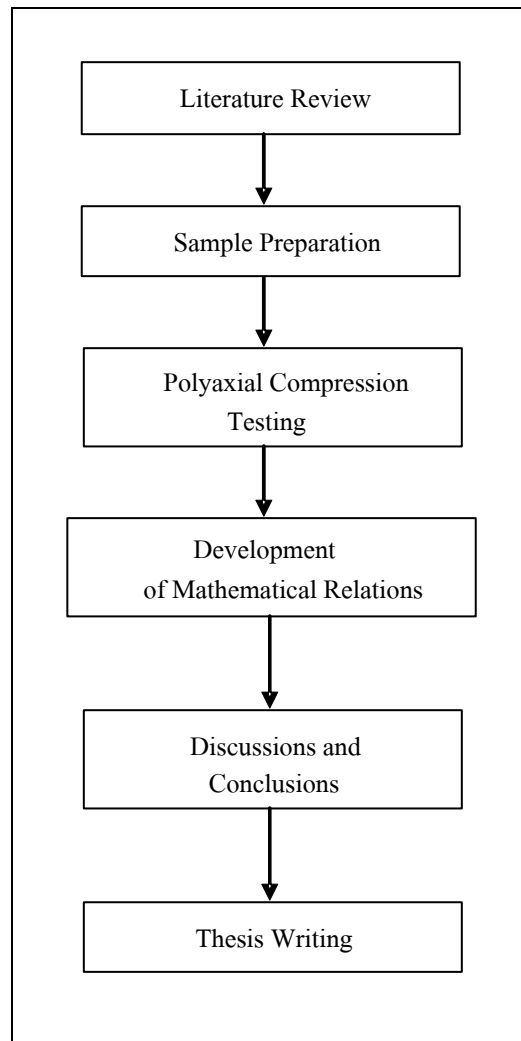
Figure 1.1 Research methodology

1.3.3 Polyaxial compressive testing

The laboratory testing includes the true triaxial compressive strength tests in polyaxial load frame. It is performed on the Phra Wihan sandstone. Their

results are used to develop a multi-axial strength criterion. Over 30 specimens are tested under various σ_1, σ_2 and σ_3 values.

1.3.4   Development of mathematical relations

Results from the laboratory measurements in terms of intermediate principal stresses and strength of rock are used to formulate a mathematical relation. Intermediate principal stresses and the applied stresses can be incorporated to the equation, and derive a new failure criterion for rocks under three dimension stress states.

1.3.5   Conclusions and thesis writing

All research activities, methods, and results are documented and complied in the thesis.

1.4   Scope and limitations

The scope and limitations of the research include as follows.

1. Laboratory experiments are conducted on rock specimens from Phra Wihan formation.

2. Testing are made under intermediate principal stress ranging from 0 to 60 MPa.

3. Up to 60 samples are tested, with the nominal sample size of $5\times5\times5$ cm^3.

4. All tests are conducted under ambient temperature.

5. Testing is made under dry condition.

6. No field testing is conducted.

1.5   Thesis contents

This research thesis is divided into six chapters. The first chapter includes background and rationale, research objectives, research methodology, and scope and limitations. Chapter II presents results of the literature review to improve an understanding of rock compressive strength as affected by the intermediate principal stress. Chapter III describes sample preparation. Chapter IV describes the polyaxial compressive strength test. Chapter V presents strength criterion. Chapter VI is the discussions, conclusions and recommendations for future studies.

CHAPTER II

LITERATURE REVIEW

2.1 Compressive strength of rock

Relevant topics and previous research results are reviewed to improve an understanding of rock compressive strength as affected by the intermediate principal stress. Summery of the review results is as follows.

Alsayed (2002) used specimens in the form of hollow cylinder specimens for simulating stress condition around the opening to study the behaviour of rock under a much wider variety of stress paths. The hollow cylinder specimens are used in conventional triaxial test cell, shown in Figure 2.1 It was developed by Hoek and Franklin (1968) and specially designed of internal of pressure loading configuration. Springwell sandstone specimens were subjected to under uniaxial, biaxial, triaxial and polyaxial compression, as well as indirect tension. The results obtained confirm the effect of the intermediate principal stress on rock failure and show that the apparent strength of rock is markedly influenced by the stress condition imposed. Multiaxial testing system can provide realistic prediction of the actual behaviour of rock and guide the formulation of more adequate numerical models.

Kwasniewski et al. (2003) use prismatic samples of medium-grained sandstone from Śląsk Colliery for testing under uniaxial compression, conventional triaxial compression and true triaxial compression conditions. Results of the studies show that confining pressure strongly inhibited dilatant behavior of rock samples tested under

Axial load

Internal pressure air bleed valve

External pressure oil inlet

External pressure air bleed valve

Internal pressure oil inlet
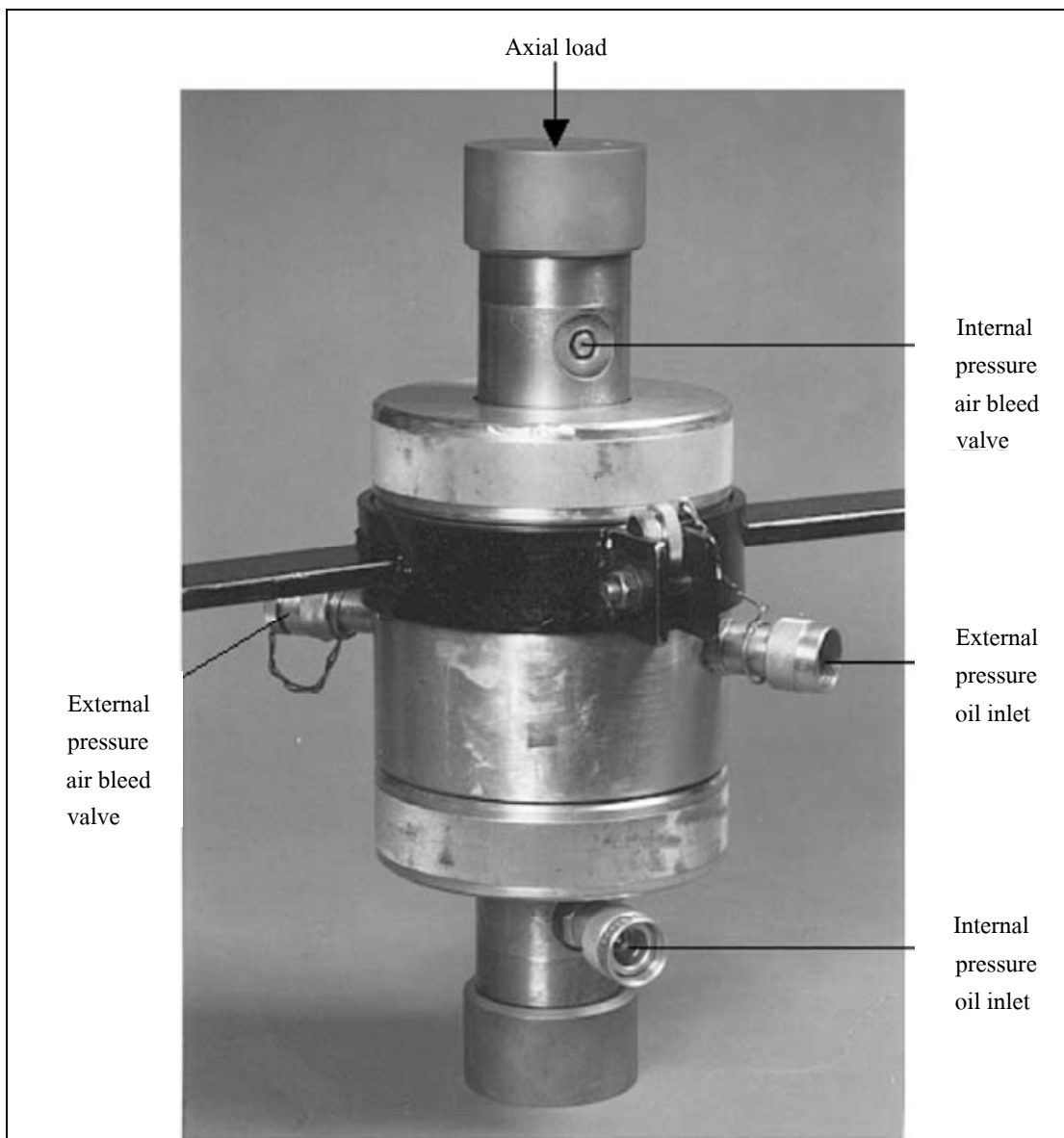
Figure 2.1 Test cell with a specimen inside ready to be transferred to the loading

machine (Alsayed, 2002).

conventional triaxial compression conditions; the increasing confinement resulted in

the growing compaction of the rock material. The effect of dilatancy was also highly

suppressed by the intermediate principal stress. While important dilatant, negative

volumetric strain corresponded to the peak differential stress at low intermediate

principal stress conditions, at high intermediate stresses the rock material was damaged to much lesser extent. As a result, faulting of rock samples in the post-peak region was much more violent and was accompanied by a strong acoustic effect.

Colmenares and Zoback (2002) examine seven different failure criteria by comparing them to published polyaxial test data ($\sigma_1 > \sigma_2 > \sigma_3$) for five different rock types at a variety of stress states. They employed a grid search algorithm to find the best set of parameters that describe failure for each criterion and the associated misfits. Overall, they found that the polyaxial criterion of Modified Wiebols and Cook and Modified Lade achieved a good fit to most of the test data. This is especially true for rocks with a highly σ_2-dependent failure behavior (e.g. Dunham dolomite, Solenhofen limestone). However, for some rock types (e.g. Shirahama Sandstone, Yuubari shale), the intermediate stress hardly affects failure and the Mohr–Coulomb and Hoek and Brown criteria fit these test data equally well, or even better, than the more complicated polyaxial criteria. The values of C_0 (uniaxial compressive strength) yielded by the Inscribed and the Circumscribed Drucker–Prager criteria bounded the C_0 (uniaxial compressive strength) value obtained using the Mohr–Coulomb criterion as expected. In general, the Drucker–Prager failure criterion did not accurately indicate the value of σ_1 at failure. The value of the misfits achieved with the empirical 1967 and 1971 the Mogi criteria were generally in between those obtained using the triaxial and the polyaxial criteria. The disadvantage of these failure criteria is that they cannot be related to strength parameters such as C_0: They also found that if only data from triaxial tests are available, it is possible to incorporate the influence of σ_2 on failure by using a polyaxial failure criterion. The results for two out of three rocks that could be analyzed in this way were encouraging.

Tiwari and Rao (2004) have described physical modeling of a rock mass under a true triaxial stress state by using block mass models having three smooth joint sets. The testing used true-triaxial system (TTS) developed by Rao and Tiwari (2002), shown in Figure 2.2 The test results show the strength of rock mass (σ_1) and deformation modulus (E_j) increase significantly which is confirmed by fracture shear planes developed on σ_2 face of specimen. Most of the specimens failed in shearing with sliding in some cases. The effect of interlocking and rotation of principal stresses σ_2 and σ_3 on strength and deformation response was also investigated

Chang and Haimson (2005) discuss the non-dilatants deformation and failure mechanism under true triaxial compression. They conducted laboratory rock strength experiments on two brittle rocks, hornfels and metapelite, which together are the major constituent of the long valley Caldera (California, USA) basement in the 2025 – 2996 m depth range. Both rocks are banded, very high porosity. Uniaxial compression test at different orientations with respect to banding planes reveal that while the hornfels compressive strength nearly isotropic, the metapelite possesses distinct anisotropy. Conventional triaxial tests in these rocks reveal that their respective strengths in a specific orientation increase approximately linearly with confining pressure. True triaxial compressive experiments in specimens oriented at a consistent angle to banding, in which the magnitude of the least (σ_3) and the intermediate (σ_2) principal stress are different but kept constant during testing while the maximum principal stress is increased until failure, exhibit a behaviour unlike that previously observed in other rocks under similar testing conditions. For a given magnitude of σ_3, compressive strength σ_1 does not vary significantly in both regardless of the applied σ_2, suggesting little or no intermediate principal stress effect.
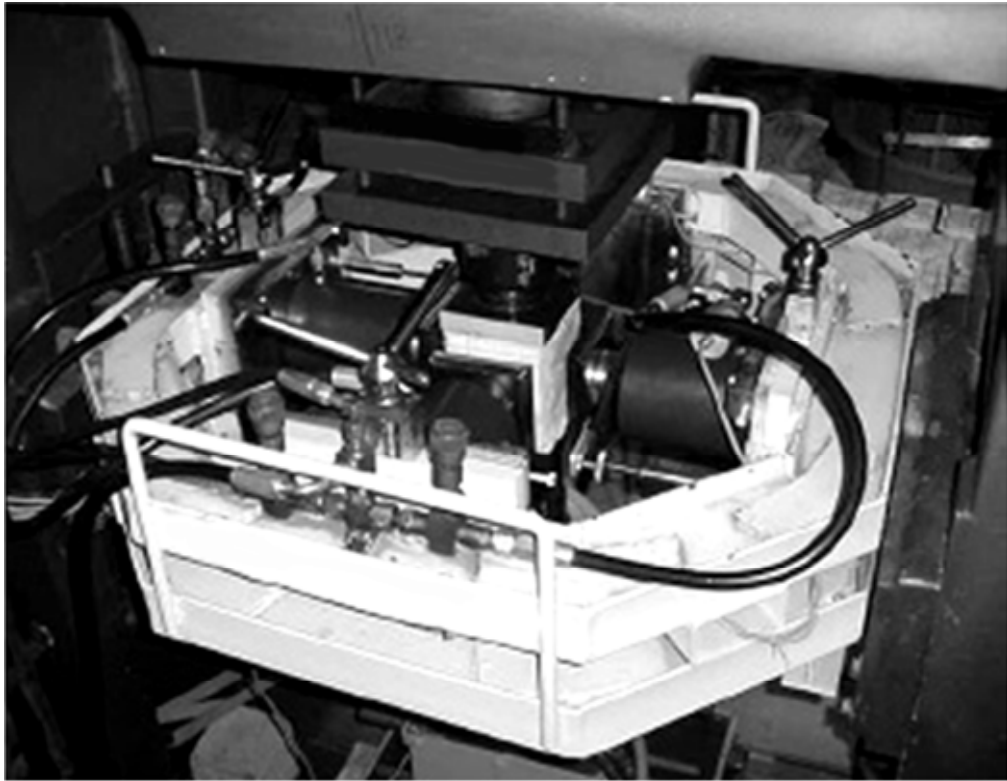
Figure 2.2 True triaxial system used for study (Rao and Tiwari, 2002).

Strains measured in all three principal directions during loading were used to obtain plots σ_1 versus volumetric strain. Theses are consistently linear almost to the point of rock failure, suggesting no dilatants.

Haimson (2006) describes the effect of the intermediate principal stress (σ_2) on brittle fracture of rocks, and on their strength criteria. Testing equipment emulating Mogi's but considerably more compact was developed at the University of Wisconsin and used for true triaxial testing of some very strong crystalline rocks. Test results revealed three distinct compressive failure mechanisms, depending on loading mode and rock type: shear faulting resulting from extensile microcrack localization, multiple splitting along the axis, and nondilatant shear failure. The true triaxial strength

criterion for the KTB amphibolite derived from such tests was used in conjunction with logged breakout dimensions to estimate the maximum horizontal in situ stress in the KTB ultra deep scientific hole.

Cai (2008) studied the intermediate principal stress on rock fracturing and strength near excavation boundaries using a FEM/ DEM combined numerical tool. A loading condition of $\sigma_3 = 0$ and $\sigma_1 \neq 0$, and $\sigma_2 \neq 0$ exists at the tunnel boundary, where σ_1, σ_2, and σ_3, are the maximum, intermediate, and minimum principal stress components, respectively. The numerical study is based on sample loading testing that follows this type of boundary stress condition. It is seen from the simulation results that the generation of tunnel surface parallel fractures and microcracks is attributed to material heterogeneity and the existence of relatively high intermediate principal stress (σ_2), as well as zero to low minimum principal stress (σ_3) confinement. A high intermediate principal stress confines the rock in such away that microcracks and fractures can only be developed in the direction parallel to σ_1 and σ_2. Stress-induced fracturing and microcracking in this fashion can lead to onion-skin fractures, spalling, and slabbing in shallow ground near the opening and surface parallel microcracks further away from the opening, leading to anisotropic behavior of the rock. Consideration of the effect of the intermediate principal stress on rock behavior should focus on the stress-induced anisotropic strength and deformation behavior of the rocks show in Figure 2.3 It is also found that the intermediate principal stress has limited influence on the peak strength of the rock near the excavation boundary.

Walsri et al. (2009) developed polyaxial load frame to determine the compressive and tensile strengths of three types of sandstone under true triaxial stresses. Results from the polyaxial compression tests on rectangular specimens of sandstones suggest
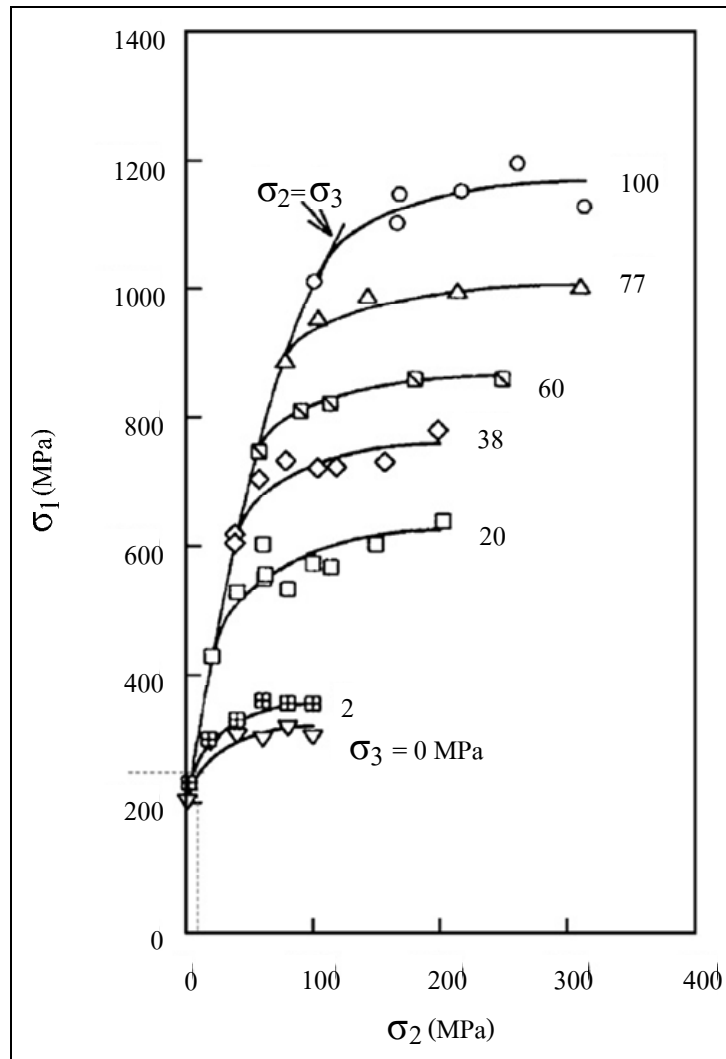
Figure 2.3 Influence of the intermediate principal stress on the strength of Westerly

granite. Rapid initial rock strength increases with increasing σ_2 can be

seen for low σ_3 (Cai, 2008).

that the rocks are transversely isotropic. The measured elastic modulus in the direction

parallel to the bedding planes is slightly greater than that normal to the bed. Poisson's

ratio on the plane normal to the bedding planes is lower than those on the parallel

ones. Under the same σ_3, σ_1 at failure increases with σ_2. Results from the Brazilian

tension tests under axial compression reveal the effects of the intermediate principal

stress on the rock tensile strength. The Coulomb and modified Wiebols and Cook failure criteria derived from the characterization test results predict the sandstone strengths in term of $J_2^{1/2}$ as a function of J_1 under true triaxial stresses. The modified Wiebols and Cook criterion describes the failure stresses better than does the Coulomb criterion when all principal stresses are in compressions. When the minimum principal stresses are in tension, the Coulomb criterion over-estimate the second order of the stress invariant at failure by about 20% while the modified Wiebols and Cook criterion fails to describe the rock tensile strengths.

2.2 Polyaxial strength criteria

In this research we aim to find which failure criterion, and parameters that best describe the behavior of rock by minimizing the mean standard deviation misfit between the predicted failure stress and the experimental data.

The Coulomb criterion indicates that when shear failure takes place across a plane, the normal stress σ_n and the shear stress τ across this plane are related by functional relation characteristics of the material

$$|\tau| = S_0 + \mu_i \sigma_n \tag{2.1}$$

where S_0 is the shear strength or cohesion of the material and μ_i is the coefficient of internal friction of the material. Since the sign of τ only affects the sliding direction, only the magnitude of τ matters. The linearzed form of the Mohr failure criterion may also be written as:

$$\sigma_1 = C_0 + q\sigma_3 \tag{2.2}$$

where: $q = \left[(\mu_i^2 + 1)^{1/2} + \mu_i^2 \right]^2 = \tan^2(\pi/4 + \varphi/2)$ (2.3)

where σ_1 is the major principal effective stress at failure, σ_3 is the least principal effective stress at failure, C_0 is the uniaxial compressive strength and ϕ is the angle of internal friction equivalent to $\tan(\mu_i)$: This failure criterion assumes that the intermediate principal stress has no influence on failure.

The Modified Wiebols and Cook criterion described by Zhou (1994) predicts that a rock fails if:

$$J_2^{1/2} = A + BJ_1 + CJ_1^2$$ (2.4)

where: $J_2^{1/2} = \sqrt{(1/6)\{(\sigma_1 - \sigma_2)^2 + (\sigma_1 - \sigma_3)^2 + (\sigma_2 - \sigma_3)^2\}}$ (2.5)

$$J_1 = (\sigma_1 + \sigma_2 + \sigma_3)/3$$ (2.6)

where J_1 is the mean effective confining stress and $J_2^{1/2} = (3/2)^{1/2}\tau_{oct}$; where τ_{oct} is the octahedral shear stress:

$$\tau_{oct} = \frac{1}{3}\sqrt{(\sigma_1 - \sigma_2)^2 + (\sigma_1 - \sigma_3)^2 + (\sigma_2 - \sigma_3)^2}$$ (2.7)

The constants A, B and C depend on rock materials and the minimum principal stresses (σ_3). They can be determined under the conditions where $\sigma_2 = \sigma_3$, as follows:

$$C = \frac{\sqrt{27}}{2C_1 + (q-1)\sigma_3 - C_0} \times \left(\frac{C_1 + (q-1)\sigma_3 - C_0}{2C_1 + (2q+1)\sigma_3 - C_0} - \frac{q-1}{q+2} \right)$$ (2.8)

where: $C_1 = (1 + 0.6\mu_i)C_0$

C_0 = uniaxial compressive strength of the rock

$\mu_i = \tan\varphi$

$q = \{(\mu_i^2 + 1)^{1/2} + \mu_i\}^2 = \tan^2(\pi/4 + \varphi/2)$

$$B = \frac{\sqrt{3}(q-1)}{q+2} - \frac{C}{3}(2C_0 + (q+2)\sigma_3$$ (2.9)

$$A = \frac{C_0}{\sqrt{3}} - \frac{C_0}{3}B - \frac{C_0^2}{9}C$$ (2.10)

The rock strength predictions produced using Eq. (2.4) are similar to that of Wiebols and Cook and thus the model described by Eq. (2.4) represents a modified strain energy criterion, which may be called Modified Wiebols and Cook. For polyaxial states of stress, the predictions made by this criterion are greater than that of the Mohr–Coulomb criterion.

Mogi (1967) empirical criterion indicates the influence of the intermediate stress on failure by performing confined compression tests ($\sigma_1 > \sigma_2 = \sigma_3$), confined extension tests ($\sigma_1 = \sigma_2 > \sigma_3$) and biaxial tests ($\sigma_1 > \sigma_2 > \sigma_3 = 0$) on different rocks. He recognized that the influence of the intermediate principal stress on failure is non-zero, but considerably smaller than the effect of the minimum principal stress. When he plotted the maximum shear stress ($\sigma_1 - \sigma_3$)/2 as a function of ($\sigma_1 + \sigma_3$)/2 for failure of Westerly Granite, he observed that the extension curve lied slightly above the compression curve and the opposite happened when he plotted the octahedral shear stress τ_{oct} as a function of the mean normal stress ($\sigma_1 + \sigma_2 + \sigma_3$)/3 for failure of the

same rock. Therefore, if ($\sigma_1 + \beta\sigma_2 + \sigma_3$) is taken as the abscissa (instead of ($\sigma_1 + \sigma_3$) or ($\sigma_1 + \sigma_2 + \sigma_3$)), the compression and the extension curves become coincidental at a suitable value of β. Mogi argued that this β value is nearly the same for all brittle rocks but we will test this assertion. The empirical criterion has the following formula:

$$(\sigma_1 - \sigma_3)/2 = f_1[(\sigma_1 + \beta\sigma_2 + \sigma_3)/2] \tag{2.11}$$

where β is a constant smaller than 1. The form of the function f_1 in Eq. (2.11) is dependent on rock type and it should be a monotonically increasing function. This criterion postulates that failure takes place when the distortional energy increases to a limiting value, which increases monotonically with the mean normal pressure on the fault plane. The term $\beta\sigma_2$ may correspond to the contribution of σ_2 to the normal stress on the fault plane because the fault surface, being irregular, is not exactly parallel to σ_2 and it would be deviated approximately by arcsin (β).

Mogi 1971 empirical criterion empirical fracture criterion was obtained by generalization of the von Mises's theory. It is formulated by:

$$\tau_{oct} = f_1(\sigma_1 + \sigma_3) \tag{2.12}$$

where f_1 is a monotonically increasing function. According to Mogi the data points tend to align in a single curve for each rock, although they slightly scatter in some silicate rocks. The octahedral stress is not always constant but increases monotonically with ($\sigma_1 + \sigma_3$). Failure will occur when the distortional strain energy reaches a critical value that increases monotonically with the effective mean pressure on the slip planes

parallel to the σ_2 direction. The effective mean pressure on faulting is $(\sigma_1 + \sigma_3)/2$ or $\sigma_{m,2}$; therefore, τ_{oct} at fracture is plotted against $\sigma_{m,2}$. Mogi applied this failure criterion to different kinds of rocks and it always gave satisfactory results.

CHAPTER III

SAMPLE PREPARATION

This chapter describes sample preparation ad specifications of the PW sandstone. The method follows as much as practical the standard practices. The tested sandstone is from Phra Wihan formation (PW sandstone). It is fine-grained quartz sandstone. It is selected primarily because of its highly uniform texture, density and strength. Its average grain size is 0.1-1.0 mm. The rock is commonly found in the north and northeast of Thailand. Its mechanical properties and responses play a significant role in the stability of tunnels, slope embankments and dam foundations in the region.

PW sandstone specimens are collected from Saraburi province. Sample preparation is carried out in the laboratory at the Suranaree University of Technology. Samples prepared for polyaxial compressive strength test are $5\times5\times5$ cm^3 shown in Figure 3.1. For the polyaxial compression testing cubical block specimens are cut and ground to have a nominal dimension of $5\times5\times5$ cm^3. This small size is to ensure that the polyaxial load frame is capable of inducing failure to the rock under confinement up to 20 MPa. A total of 59 specimens are prepared for testing. Table 3.1 summarizes the specimen number, dimension and density.

Figure 3.1 Some PW sandstone specimens prepared for polyaxial

compression testing.

Table 3.1 Specimen dimensions after preparation.

Specimen No.	Width (mm.)	Length (mm.)	Height (mm.)	Density (g/cc)
PWSS-PX-01	53.25	53.03	50.60	2.27
PWSS-PX-02	51.30	51.05	50.00	2.42
PWSS-PX-03	51.05	50.83	51.30	2.30
PWSS-PX-04	51.51	51.29	48.72	2.46
PWSS-PX-05	51.87	51.65	50.04	2.34
PWSS-PX-06	50.61	50.39	51.60	2.32
PWSS-PX-07	50.25	50.03	51.66	2.27
PWSS-PX-08	50.75	50.53	49.99	2.37
PWSS-PX-09	50.15	49.93	50.30	2.34
PWSS-PX-10	50.70	50.48	51.21	2.33
PWSS-PX-11	51.83	51.61	50.80	2.35
PWSS-PX-12	50.36	50.14	50.71	2.34
PWSS-PX-13	51.35	51.13	51.85	2.21
PWSS-PX-14	49.75	49.53	50.45	2.34
PWSS-PX-15	51.67	51.45	50.73	2.32
PWSS-PX-16	50.45	50.23	51.00	2.35
PWSS-PX-17	52.21	51.99	49.85	2.44
PWSS-PX-18	50.55	50.33	51.51	2.32
PWSS-PX-19	52.00	51.78	51.35	2.25
PWSS-PX-20	51.00	50.78	52.75	2.30
PWSS-PX-21	50.72	50.5	50.85	2.36
PWSS-PX-22	50.58	50.36	51.53	2.27
PWSS-PX-23	51.13	50.91	50.34	2.31
PWSS-PX-24	50.63	50.41	52.00	2.37
PWSS-PX-25	50.95	50.73	51.00	2.32
PWSS-PX-26	51.25	51.03	50.14	2.37
PWSS-PX-27	50.50	50.28	52.00	2.33
PWSS-PX-28	50.75	50.53	50.75	2.35
PWSS-PX-29	50.40	50.18	50.00	2.34
PWSS-PX-30	50.00	49.78	51.05	2.32
PWSS-PX-31	50.65	50.43	51.08	2.30
PWSS-PX-32	51.15	50.93	50.25	2.38
PWSS-PX-33	51.30	51.08	50.90	2.29
PWSS-PX-34	50.53	50.31	50.98	2.30
PWSS-PX-35	51.44	51.22	51.70	2.25
PWSS-PX-36	51.30	51.08	50.65	2.26
PWSS-PX-37	50.20	49.98	51.30	2.31

Table 3.1 Specimen dimensions after preparation (cont.).

Specimen No.	Width (mm.)	Length (mm.)	Height (mm.)	Density (g/cc)
PWSS-PX-38	50.29	50.07	50.30	2.39
PWSS-PX-39	50.49	50.27	50.81	2.36
PWSS-PX-40	50.26	50.04	51.40	2.28
PWSS-PX-41	50.06	49.84	51.30	2.29
PWSS-PX-42	50.95	50.73	50.85	2.33
PWSS-PX-43	51.69	51.47	51.14	2.26
PWSS-PX-44	51.01	50.79	50.10	2.35
PWSS-PX-45	51.19	50.97	50.69	2.24
PWSS-PX-46	50.68	50.46	50.80	2.24
PWSS-PX-47	50.44	50.22	50.56	2.34
PWSS-PX-48	50.43	50.21	51.29	2.35
PWSS-PX-49	50.73	50.51	51.10	2.31
PWSS-PX-50	50.53	50.31	51.14	2.35
PWSS-PX-51	51.08	50.86	51.04	2.34
PWSS-PX-52	50.83	50.61	50.13	2.41
PWSS-PX-53	51.28	51.06	50.28	2.39
PWSS-PX-54	51.31	51.09	50.20	2.35
PWSS-PX-55	50.58	50.36	50.65	2.35
PWSS-PX-56	49.23	49.01	50.01	2.37
PWSS-PX-57	50.65	50.43	50.25	2.39
PWSS-PX-58	51.65	51.43	50.59	2.44
PWSS-PX-59	51.25	51.03	50.48	2.33

CHAPTER IV

POLYAXIAL COMPRESSIVE STRENGTH TESTS

4.1   Introduction

The objective of this chapter is to experimentally determine the compressive strengths of Phra Wihan sandstone (PW sandstone) subjected to anisotropic stress states. This chapter describes the equipment, method, results and analysis of the polyaxial compressive strength tests on the rock. A total of 22 specimens have been tested.

4.2   Test equipment

Figure 4.1 shows the polyaxial load frame (Walsri et al., 2009) used in this test. The polyaxial compression tests are performed to determine the compressive strengths and deformations of the PW sandstone under true triaxial stresses. The intermediate (σ_2) and minimum (σ_3) principal stresses are maintained constant while σ_1 is increased until failure. Here the constant σ_2 is varied from 6.6 to 60 MPa, and σ_3 from 2.3 to 15 MPa. Neoprene sheets are used to minimize the friction at all interfaces between the loading platen and the rock surface. Figure 4.2 shows the applied principal stress directions with respect for all specimens. The failure stresses are recorded and mode of failure examined. To meet the load requirement above, two pairs of cantilever beams are used to apply the lateral stresses in mutually perpendicular directions on the specimen. The outer end of each opposite beam is pulled down by dead weight placed in the middle of a steel bar linking the
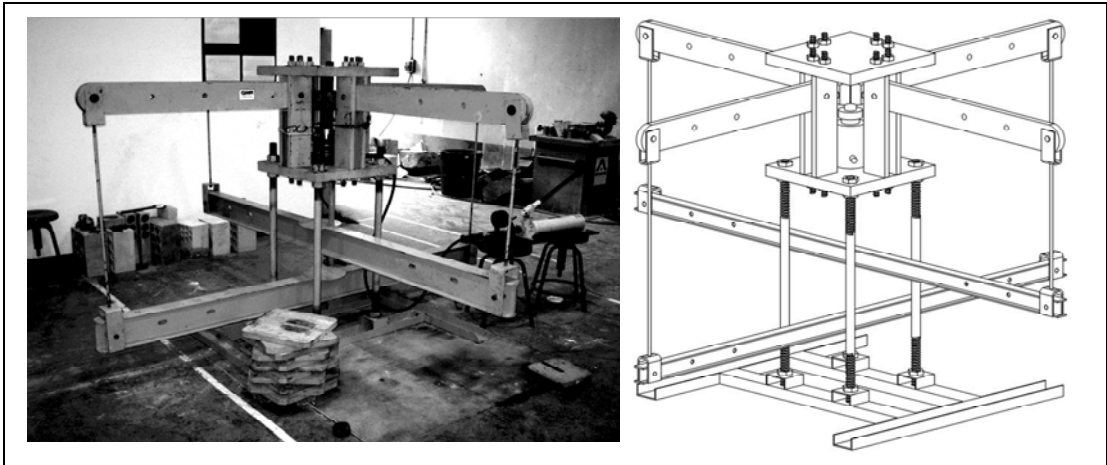
Figure 4.1 Polyaxial load frame developed for compressive strength testing under true triaxial stresses (from Walsri et al., 2009).
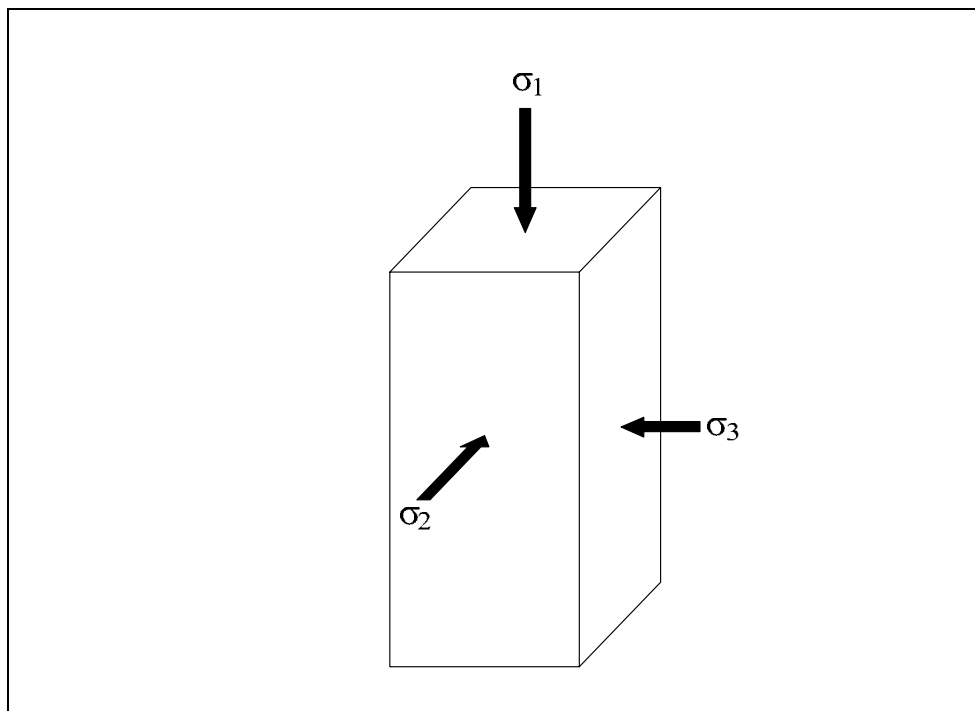

Figure 4.2 Directions of loading on cubical specimens of sandstone.

two opposite beams underneath (Figure 4.3). The inner end is hinged by a pin mounted on vertical bars on each side of the frame. During testing all beams are arranged perfectly horizontally, and hence a lateral compressive load results on the specimen placed at the center of the frame. Due to the different distances from the pin to the outer weighting point and from the pin to the inner loading point, a load magnification of 17 to 1 is obtained from load calibration with an electronic load cell. This loading ratio is also used to determine the lateral deformation of the specimen by monitoring the vertical movement of the two steel bars below. The maximum lateral load is designed for 100 kN. The axial load is applied by a 1000-kN hydraulic load cell. The load frame can accommodate specimen sizes from 2.5×2.5×2.5 to 10×10×20 cm^3. The different specimen sizes and shapes can be tested by adjusting the distances between the opposite loading platens. Note that virtually all true triaxial and polyaxial cells previously developed elsewhere can test rock samples with the maximum size not larger than 5×5×10 cm^3. σ_1 is obtained from the maximum stresses failure. σ_2 and σ_3 are obtained from calibration by load cell. Figure 4.4 plots the calibrated curves for use in polyaxial compression test. F is load on the rock sample (kN). W is weight on the lower bars (kN).

4.3 Test method

The prepared rock specimen has a nominal dimension of 5×5×5 cm^3. The test produce can be described as follows:

1) Use neoprene sheet on six sides of rock specimen.

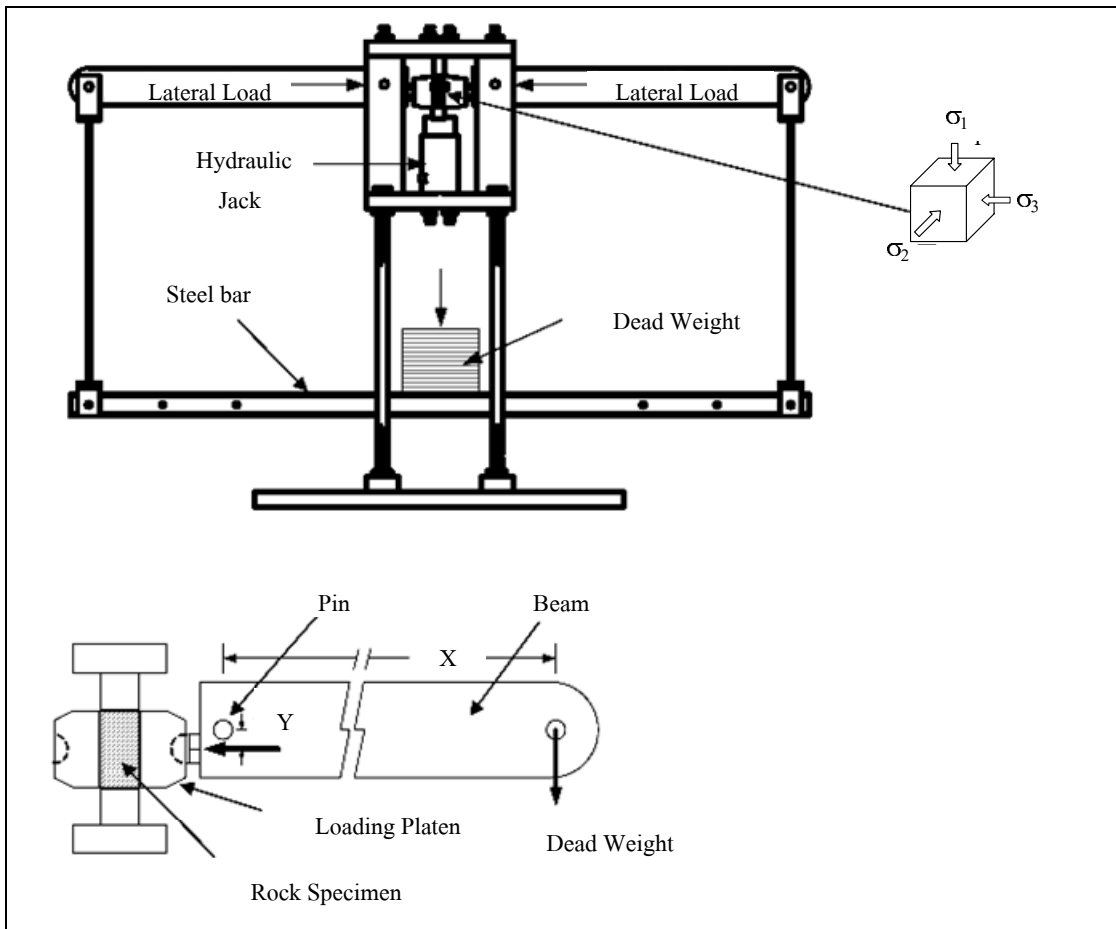2) Connect hydraulic pump with hydraulic cylinder and check level of oil in the pump.

Figure 4.3 Cantilever beam weighed at outer end applies lateral stress to the rock
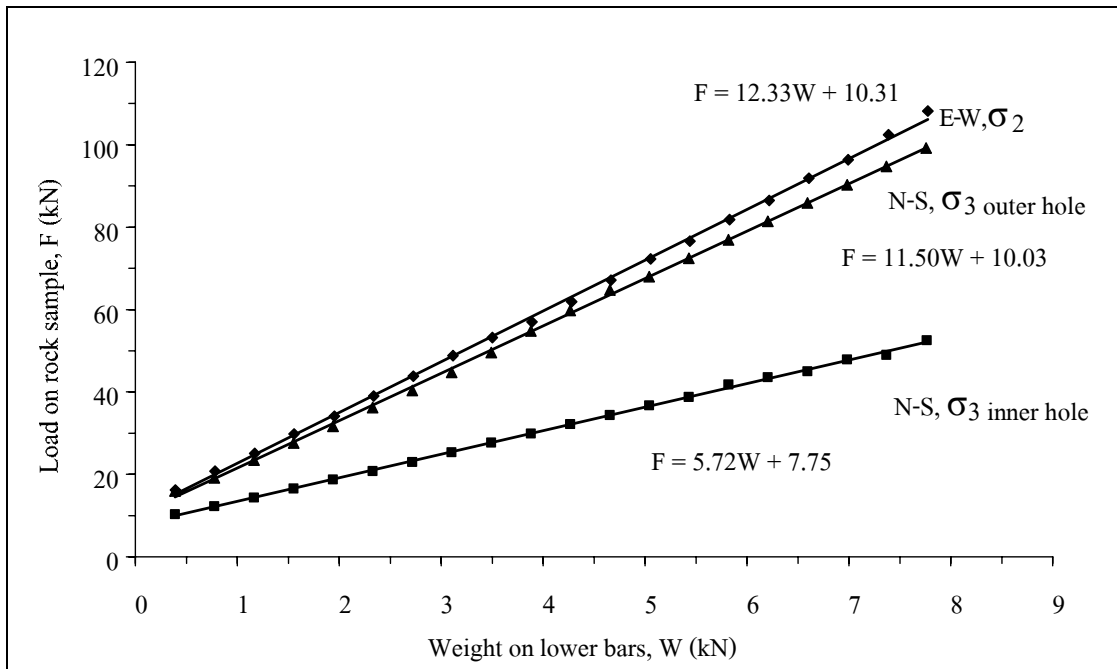
specimen (from Walsri et al., 2009).

Figure 4.4 Calibrated curves for use in polyaxial compression testing.

3) The rock specimen with neoprene is placed on the loading platen.

4) The lateral loading platens contact the sides of specimen.

5) Raise the cantilever beam in N–S direction.

6) Place the rock specimen with neoprene and lateral loading platen into the polyaxial load frame.

7) Lateral loading platens must be straight with half spherical bolt.

8) Slowly reduce the level of cantilever beam until half spherical bolts and lateral loading platen are in contact.

9) Raise the cantilever beam in W–E direction.

10) Place the lateral loading platens on the sides of specimen.

11) Slowly reduce level of the cantilever beam.

12) Place the loading platens on top and bottom of the specimen.

13) Increase oil pressure using hydraulic pump until specimen, loading platens and upper steel plates are in contact.

14) If confining pressure is highs than 4.1 kN, use inner hole to hang the lower bars, 6.5 kN outer hole of lateral loading platens install the lower beam in N–S direction with U-links for carry dead weight by using steel bolts.

15) Put a steel plate (dead weight) on the middle of each beam to increase lateral load.

16) Axial load and lateral load must be increased simultaneously up to pre-set pressure so that rock specimen will be in hydrostatic condition.

17) Install dial gages in monitoring directions.

4.4   Test results

This section describes test results in terms of strength and elasticity. The measured sample deformations are used to determine the strains along the principal axes during loading. The failure stresses are recorded and mode of failure examined. Appendix A shows the stress-strain curves from the start of loading to failure for the sandstone specimens in true triaxial stress states.

4.4.1   Strength results

Table 4.1 summarizes the strengths with respect to the orientation of the true triaxial compression stresses. Figure 4.5 plots σ_1 at failure as a function of σ_2 tested under various σ_3's for PW sandstone. The results show the effects of the intermediate principal stress, σ_2, on the maximum stresses at failure by the failure envelopes being offset from the condition where $\sigma_2 = \sigma_3$. For all minimum principal stress levels, σ_1 at failure increases with σ_2. The effect of σ_2 tends to be more

pronounced under a greater σ_3. These observations agree with those obtained elsewhere (e.g. Haimson and Chang, 1999; Colmenares and Zoback, 2002; Haimson, 2006). Post-failure observations suggest that compressive shear failures are predominant in the specimens tested under low σ_2 while splitting tensile fractures parallel to σ_1 and σ_2 directions dominate under higher σ_2 (Figure 4.6). The observed splitting tensile fractures under relatively high σ_2 suggest that the fracture initiation has no influence from the friction at the loading interface in the σ_2 direction. As a result the increase of σ_1 with σ_2 should not be due to the interface friction.

Figures 4.7 (results of triaxial compressive strength from polyaxial compressive strength tests in terms of Mohr's circles and Coulomb criterion) shows the Mohr circles of the results with shear stress as ordinates and normal stress as

Table 4.1 Summary of the strength results on PW sandstone of true triaxial compression tests.

Specimen No.	σ_3 (MPa)	σ_2 (MPa)	σ_1 (MPa)
PWSS-PX-38		10.0	80.3
PWSS-PX-03	2.3	20.0	100.3
PWSS-PX-58		40.0	117.4
PWSS-PX-55		60.0	117.4
PWSS-PX-44		10.0	95.0
PWSS-PX-08	4.1	20.0	109.5
PWSS-PX-27		40.0	124.8
PWSS-PX-01		60.0	131.2
PWSS-PX-42	6.5	6.6	94.5
PWSS-PX-30		10.0	106.6
PWSS-PX-33	6.6	20.0	118.0
PWSS-PX-45		40.0	141.1
PWSS-PX-02		60.0	150.2
PWSS-PX-21	8.3	8.3	108.9
PWSS-PX-23	10.0	10.1	125.1
PWSS-PX-34		20.0	135.0
PWSS-PX-35	10.1	30.0	147.1
PWSS-PX-32		40.0	161.2
PWSS-PX-49		50.0	172.0
PWSS-PX-29	12.0	12.0	139.2
PWSS-PX-37	15.5	15.5	147.4
PWSS-PX-46	20.0	20.0	161.9
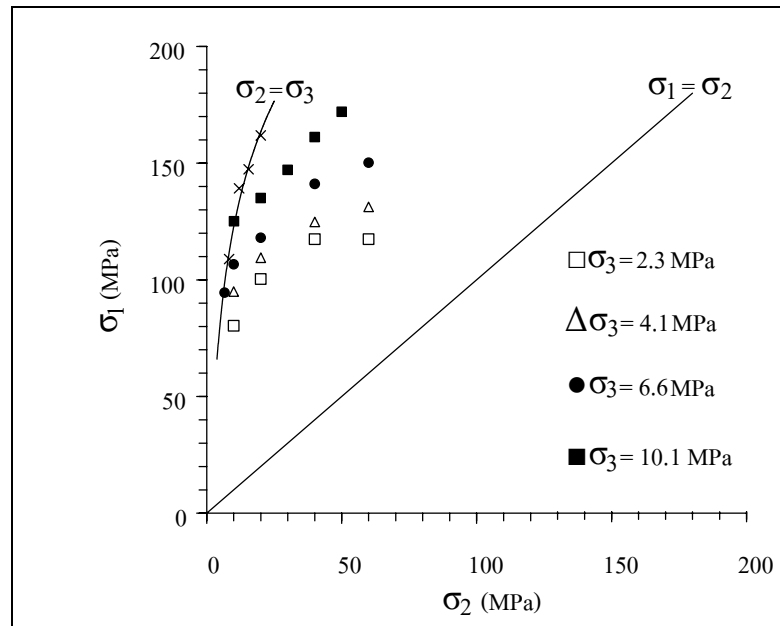
Figure 4.5 Maximum principal stresses (σ_1) at failure as a function of σ_2 for various
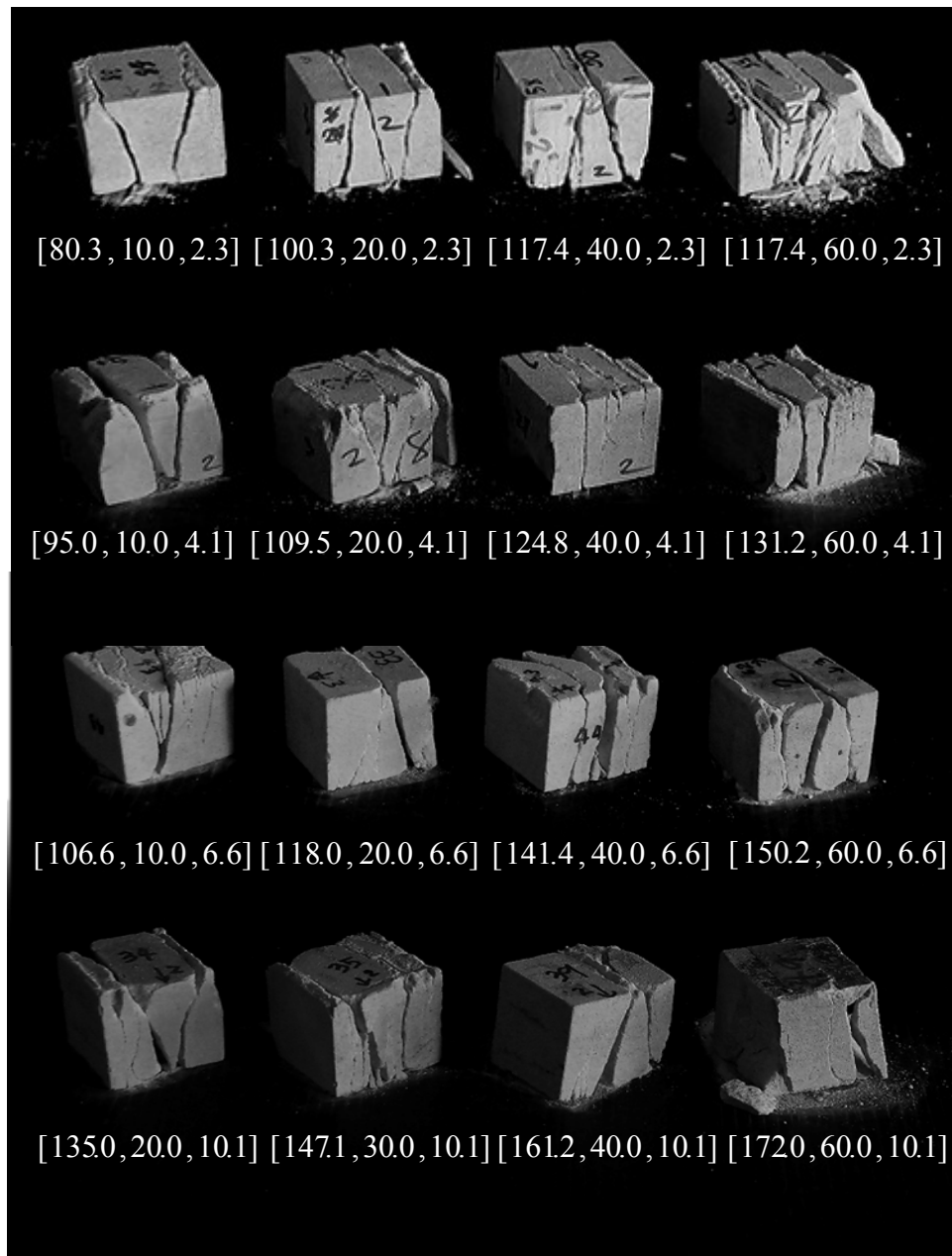
σ_3 values.

Figure 4.6 Some post-test specimens of PW sandstone. Numbers in blankets indicate

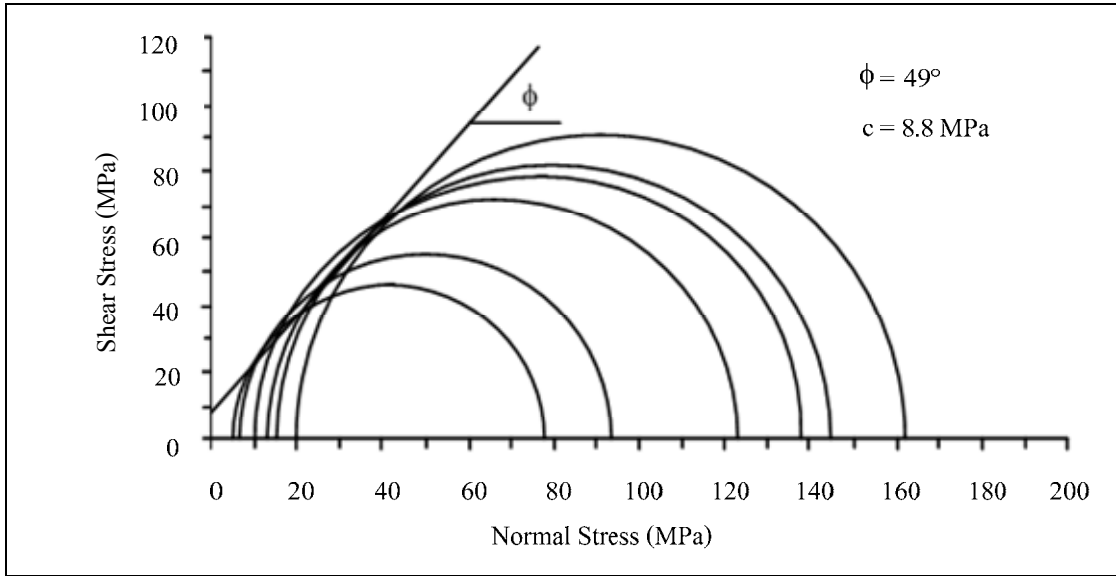$[\sigma_1, \sigma_2, \sigma_3]$ at failure.

Figure 4.7 Results of triaxial compressive strength from polyaxial compressive
strength tests in terms of the Mohr's circles and Coulomb criterion.

abscissas. The relationship can be represented by the Coulomb criterion:

$$\tau = c + \sigma_n \tan\phi \qquad (4.1)$$

where τ is the shear stress, c is the cohesion, σ_n is the normal stress and ϕ is the angle
of internal friction. The friction angle = 49° and the cohesion = 8.8 MPa.

4.4.2 Elastic results

The elastic modulus and Poisson's ratio are calculated for the three-dimensional principal stress-strain relations, given by Jaeger and Cook (1979). The
relation can be simplified to obtain a set of governing equations for an isotropic
material as follows:

$$\varepsilon_1 = \frac{\sigma_1}{E} - \frac{v}{E}(\sigma_2 + \sigma_3) \qquad (4.2)$$

$$\varepsilon_2 = \frac{\sigma_2}{E} - \frac{\nu}{E}(\sigma_1 + \sigma_3) \qquad (4.3)$$

$$\varepsilon_3 = \frac{\sigma_3}{E} - \frac{\nu}{E}(\sigma_1 + \sigma_2) \qquad (4.4)$$

$$\varepsilon_v = \varepsilon_1 + \varepsilon_2 + \varepsilon_3 \qquad (4.5)$$

where σ_1, σ_2 and σ_3 are principal stresses, ε_1, ε_2 and ε_3 are principal strains, ε_v are volumetric strain, E is elastic modulus, and ν is Poisson's ratio.

$$\varepsilon_1 = \frac{\Delta d_1}{d_1} \qquad (4.6)$$

$$\varepsilon_2 = \frac{\Delta d_2}{d_2} \qquad (4.7)$$

$$\varepsilon_3 = \frac{\Delta d_3}{d_3} \qquad (4.8)$$

$$E_{12} = \left[\frac{\sigma_1}{\varepsilon_1} - \frac{\nu_{12}}{\varepsilon_1}(\sigma_2 + \sigma_3)\right] + \left[\frac{\sigma_2}{\varepsilon_2} - \frac{\nu_{12}}{\varepsilon_2}(\sigma_1 + \sigma_3)\right] \qquad (4.9)$$

$$E_{13} = \left[\frac{\sigma_1}{\varepsilon_1} - \frac{\nu_{13}}{\varepsilon_1}(\sigma_2 + \sigma_3)\right] + \left[\frac{\sigma_3}{\varepsilon_3} - \frac{\nu_{13}}{\varepsilon_3}(\sigma_1 + \sigma_2)\right] \qquad (4.10)$$

$$E_{23} = \left[\frac{\sigma_2}{\varepsilon_2} - \frac{\nu_{23}}{\varepsilon_2}(\sigma_1 + \sigma_3)\right] + \left[\frac{\sigma_3}{\varepsilon_3} - \frac{\nu_{23}}{\varepsilon_3}(\sigma_1 + \sigma_2)\right] \qquad (4.11)$$

$$\nu_{12} = \left[\frac{\varepsilon_1 E_{12} + \sigma_1}{\sigma_2 + \sigma_3}\right] + \left[\frac{\varepsilon_2 E_{12} + \sigma_2}{\sigma_1 + \sigma_3}\right] \qquad (4.12)$$

$$\nu_{13} = \left[\frac{\varepsilon_1 E_{13} + \sigma_1}{\sigma_2 + \sigma_3}\right] + \left[\frac{\varepsilon_3 E_{13} + \sigma_3}{\sigma_1 + \sigma_2}\right] \qquad (4.13)$$

$$\nu_{23} = \left[\frac{\varepsilon_2 E_{23} + \sigma_2}{\sigma_1 + \sigma_3}\right] + \left[\frac{\varepsilon_3 E_{23} + \sigma_3}{\sigma_1 + \sigma_2}\right] \qquad (4.14)$$

The calculations of the Poisson's ratios and tangent elastic moduli are made at 50% of the maximum principal stress. Table 4.2 summarizes the elastic parameters with respect to the orientation of the true triaxial compression tests.

Table 4.2 Summary of the elastic parameters with respect to the orientation of the

principal axes.

Specimen No.	Elastic Modulus (GPa)				Poisson's ratio			
	E_{12}	E_{13}	E_{23}	Average	v_{12}	v_{13}	v_{23}	Average
PWSS-PX-38	7.67	8.63	13.32	9.87	0.31	0.21	0.33	0.28
PWSS-PX-03	10.66	10.77	10.83	10.75	0.25	0.24	0.25	0.25
PWSS-PX-58	10.35	11.27	11.04	10.89	0.29	0.24	0.23	0.25
PWSS-PX-55	10.19	11.28	10.74	10.74	0.33	0.26	0.23	0.28
PWSS-PX-44	8.12	8.67	15.07	10.62	0.30	0.20	0.20	0.23
PWSS-PX-08	8.94	10.59	10.08	9.87	0.30	0.21	0.33	0.28
PWSS-PX-27	10.32	12.83	12.48	11.88	0.25	0.27	0.22	0.25
PWSS-PX-01	8.88	12.13	11.21	10.74	0.33	0.21	0.26	0.27
PWSS-PX-42	9.17	9.20	-	9.19	0.28	0.26	-	0.27
PWSS-PX-30	10.94	11.27	10.14	10.78	0.29	0.24	0.23	0.25
PWSS-PX-33	9.08	9.20	15.15	11.14	0.32	0.22	0.32	0.28
PWSS-PX-45	8.83	11.72	12.21	10.92	0.33	0.24	0.31	0.28
PWSS-PX-02	9.27	10.70	12.18	10.72	0.32	0.22	0.26	0.27
PWSS-PX-21	9.51	9.10	-	9.31	0.26	0.26	-	0.26
PWSS-PX-23	9.59	9.74	-	9.67	0.28	0.28	-	0.28
PWSS-PX-34	9.95	11.45	10.06	10.49	0.24	0.21	0.27	0.24
PWSS-PX-35	9.34	9.87	9.60	9.60	0.25	0.21	0.25	0.24
PWSS-PX-32	9.32	10.28	8.11	9.24	0.28	0.25	0.28	0.27
PWSS-PX-49	9.32	12.17	10.67	10.72	0.30	0.23	0.26	0.27
PWSS-PX-29	9.85	9.81	-	9.83	0.27	0.28	-	0.28
PWSS-PX-37	10.33	10.33	-	10.33	0.26	0.26	-	0.26
PWSS-PX-46	9.56	9.53	-	9.55	0.28	0.28	-	0.28
Mean ± S.D.	10.31±0.71				0.26±0.02			

Note: - is not calculated because $\sigma_2 = \sigma_3$.

CHAPTER V

STRENGTH CRITERIA

5.1 Introduction

This chapter describes the strength analysis and compressive failure criteria under true triaxial compression. The test results are compared against the Coulomb and modified Wiebols and Cook failure criteria. They are selected because the Coulomb criterion has been widely used in actual field applications while the modified Wiebols and Cook criterion has been claimed by many researchers to be one of the best representations of rock strengths under confinements.

5.2 The Coulomb criterion

The second order stress invariant ($J_2^{1/2}$) and the first order stress invariant or the mean stress (J_1) is calculated from the test results by the following relations (Jaeger and Cook, 1979):

$$J_2^{1/2} = \sqrt{(1/6)\{(\sigma_1 - \sigma_2)^2 + (\sigma_1 - \sigma_3)^2 + (\sigma_2 - \sigma_3)^2\}} \qquad (5.1)$$

$$J_1 = (\sigma_1 + \sigma_2 + \sigma_3)/3 \qquad (5.2)$$

The Coulomb criterion in from of J_2 and J_1 can be expressed as (Jaeger and Cook, 1979):

$$J_2^{1/2} = \frac{2}{\sqrt{3}} \left[J_1 \sin\phi + S_0 \cos\phi \right] \tag{5.3}$$

where ϕ is friction angle, S_o is cohesion, J_1 is mean stress and $J_2^{1/2}$ is the second order of stress invariant. The uniaxial and triaxial test results indicate that the friction angle of the tested sandstone is 49°, and the cohesion is 8.8 MPa. Table 5.1 shows the results of the strength calculation in terms of $J_2^{1/2}$ and J_1 for PW sandstone. Figures 5.1 compares the polyaxial test results with those predicted by the Coulomb criterion. The predictions are made for σ_3 = 2.3, 4.1, 6.6, 8.3, 10.1, 12.0, 15.5 and 20.0 MPa. (as used in the tests) and under stress conditions from $\sigma_2 = \sigma_3$ to $\sigma_2 > \sigma_3$. In the $J_2^{1/2}$ - J_1 diagram, $J_2^{1/2}$ increases with σ_3 but it is independent of J_1 because the Coulomb criterion ignores σ_2 in the strength calculation. Under a low σ_2 and σ_3 the Coulomb prediction tends to agree with the test results obtained from the PW sandstone. Except for this case, no correlation between the Coulomb predictions and the polyaxial strengths can be found. The inadequacy of the predictability of Coulomb criterion under polyaxial stress states obtained here agrees with a conclusion drawn by Colmenares and Zoback (2002).

5.3   The Modified Wiebols and Cook criteria

The modified Wiebols and Cook criterion given by Colmenares and Zoback (2002) defines $J_2^{1/2}$ at failure in terms of J_1 as:

$$J_2^{1/2} = A + BJ_1 + CJ_1^2 \tag{5.4}$$

The constants A, B and C depend on rock materials and the minimum principal stresses (σ_3). They can be determined under the conditions where $\sigma_2 = \sigma_3$, as follows (Colmenares and Zoback, 2002):

Table 5.1 Strength calculation in terms of $J_2^{1/2}$ and J_1.

| Specimen No.	σ_3 (MPa)	σ_2 (MPa)	σ_1 (MPa)	$J_2^{1/2}$ (MPa)	J_1 (MPa)
PWSS-PX-38		10.0	80.3	43.0	30.9
PWSS-PX-03	2.3	20.0	100.3	52.2	40.9
PWSS-PX-58		40.0	117.4	58.7	53.2
PWSS-PX-55		60.0	117.4	57.6	59.9
PWSS-PX-44		10.0	95.0	50.9	36.4
PWSS-PX-08	4.1	20.0	109.5	56.8	44.5
PWSS-PX-27		40.0	124.8	62.0	56.3
PWSS-PX-01		60.0	131.2	63.7	65.1
PWSS-PX-42	6.5	6.6	94.5	50.8	35.9
PWSS-PX-30		10.0	106.6	56.8	41.1
PWSS-PX-33	6.6	20.0	118.0	60.8	48.2
PWSS-PX-45		40.0	141.1	70.0	62.6
PWSS-PX-02		60.0	150.2	72.6	72.3
PWSS-PX-21	8.3	8.3	108.9	50.2	37.3
PWSS-PX-23	10.0	10.1	125.1	66.4	48.4
PWSS-PX-34		20.0	135.0	69.4	55.0
PWSS-PX-35	10.1	30.0	147.1	74.0	62.4
PWSS-PX-32		40.0	161.2	80.0	70.4
PWSS-PX-49		50.0	172.0	84.3	77.4
PWSS-PX-29	12.0	12.0	139.2	73.5	54.4
PWSS-PX-37	15.5	15.5	147.4	76.2	59.5
PWSS-PX-46	20.0	20.0	161.9	81.9	67.3
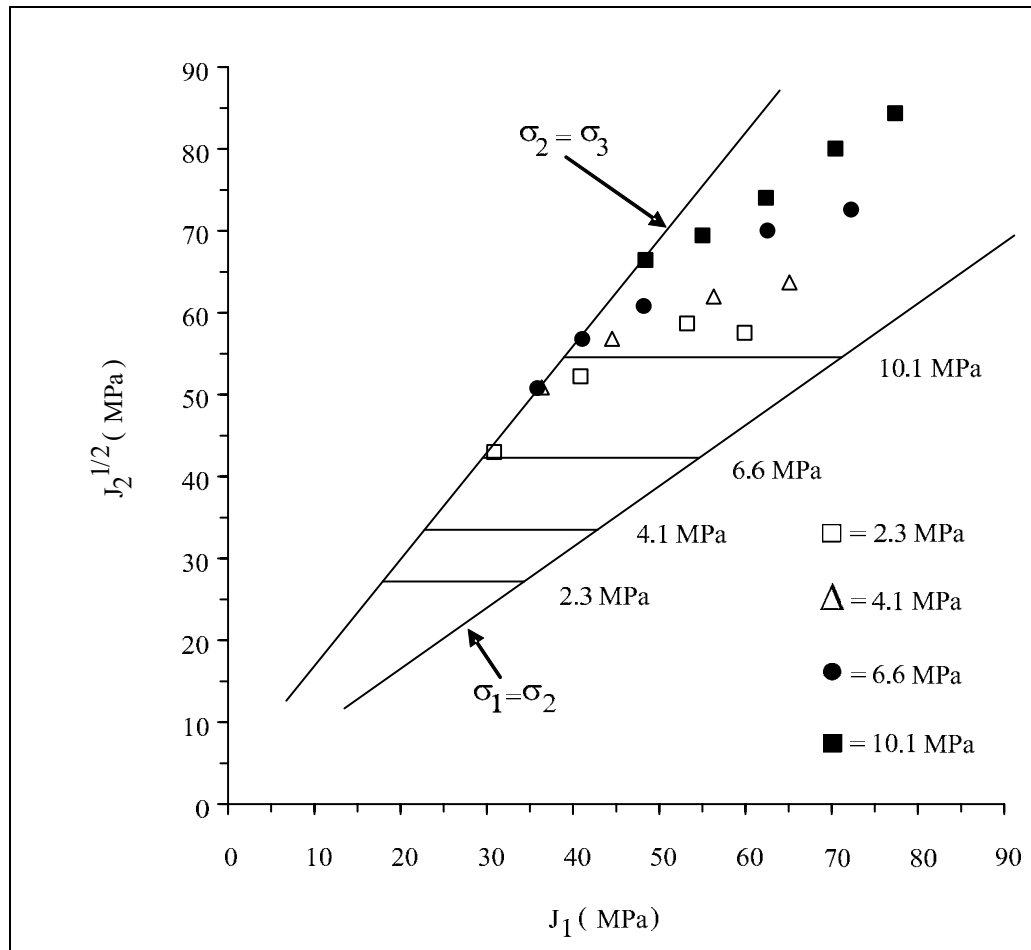
Figure 5.1 $J_2^{1/2}$ as a function of J_1 from testing PW sandstone compared with the Coulomb criterion predictions (lines).

$$C = \frac{\sqrt{27}}{2C_1 + (q-1)\sigma_3 - C_0} \times \left(\frac{C_1 + (q-1)\sigma_3 - C_0}{2C_1 + (2q+1)\sigma_3 - C_0} - \frac{q-1}{q+2} \right) \qquad (5.5)$$

where: $C_1 = (1 + 0.6\mu_i)C_0$

C_0 = uniaxial compressive strength of the rock

$\mu_i = \tan\varphi$

$q = \{(\mu_i^2 + 1)^{1/2} + \mu_i\}^2 = \tan^2(\pi/4 + \varphi/2)$

$$B = \frac{\sqrt{3}(q-1)}{q+2} - \frac{C}{3}(2C_0 + (q+2)\sigma_3) \qquad (5.6)$$

$$A = \frac{C_0}{\sqrt{3}} - \frac{C_0}{3}B - \frac{C_0^2}{9}C \qquad (5.7)$$

The numerical values of A, B and C for PW sandstones are given in Table 5.2 for each σ_3 tested. Substituting these constants into equation (5.4), the upper and lower limits of $J_2^{1/2}$ for each rock type can be defined under conditions of $\sigma_2 = \sigma_3$ and $\sigma_1 = \sigma_2$. The predictions are made for $\sigma_3 = 2.3, 4.1, 6.6, 8.3, 10.1, 12.0, 15.5$ and 20.0 MPa. Figure 5.2 compares the test results with those predicted by the modified Wiebols and Cook criterion. The predictions agree well with the test results. This conforms to the results obtained by Colmenares and Zoback (2002). The predictive capability of the modified Wiebols and Cook criterion can be improved as the minimum principal stress increases.

Table 5.2 Modified Wiebols and Cook parameters for PW sandstone.

| σ_3 (MPa) | Modified Wiebols and Cook parameters | | |
	A (MPa)	B	C (MPa^{-1})
2.3	4.311	1.706	-0.013
4.1	3.910	1.701	-0.012
6.6	3.486	1.697	-0.010
10.1	3.053	1.694	-0.008
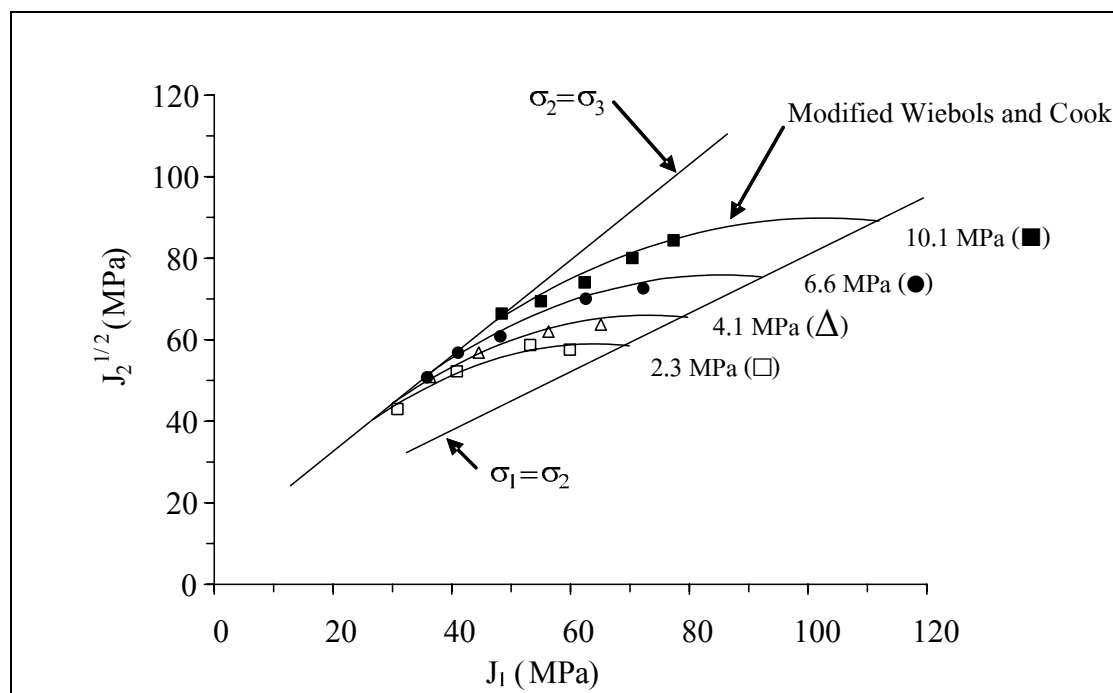
Figure 5.2 $J_2^{1/2}$ as a function of J_1 from testing PW sandstone compared with the modified Wiebols & Cook criterion predictions (lines).

5.4   Predictability of the strength criteria

The three-dimensional strength criteria are used to compare against the strength data in form of the octahedral shear strength as a function of mean stress, and the major principal stress at failure as a function of the intermediate principal stress. The mean misfit ($\bar{s}$) is determined for each criterion using as equation (Riley et al., 1998):

$$\bar{s} = \frac{1}{m}\sum_i s_i \tag{5.8}$$

where $s_i = \sqrt{\frac{1}{n}\sum_j (\sigma_{1.j}^{calc} - \sigma_{1.j}^{test})^2}$

$\sigma_{1.j}^{calc}$ = maximum stress predicted from strength criterion

$\sigma_{1.j}^{test}$ = maximum stress from test data

n　　= number of data points calculated

m　　= number of data sets

The effect of σ_2 on the PW sandstone strengths can be best described by the modified Wiebols and Cook criterion with the mean misfit = 2.93 MPa. The Coulomb criteria can not describe the PW sandstone strengths beyond the condition where $\sigma_2 = \sigma_3$, as he can not incorporate the effects of σ_2, mean misfit = 51.65 MPa.

5.5　　Discussions of the test results

Under true triaxial compressive stresses the modified Wiebols and Cook criterion can predict the compressive strengths of the tested sandstones reasonably well. This agrees with the results obtained by Haimson (2000) and Colmenares and Zoback (2002). Due to the effect of σ_2 the Coulomb criterion can not represent the rock strengths under true triaxial compressions, particularly under high σ_2 to σ_3 ratios. This is because the Coulomb criterion ignores the intermediate principal stress in the calculation of stress state at failure.

CHAPTER VI

DISCUSSIONS, CONCLUSIONS, AND

RECOMMENDATIONS FOR FUTURE STUDIES

6.1   Discussions and conclusions

True triaxial compressive strengths of PW sandstone have been determined in this study. Cubical specimens with a nominal dimension of $5 \times 5 \times 5$ cm^3 are tested. A polyaxial load frame equipped with cantilever beam is used to apply constant σ_2 and σ_3 while σ_1 (along the long axis is increased until failure. The strength results clearly show that σ_2 affects the maximum stress, σ_1, at failure for all confining pressures. This phenomenon agrees with those observed elsewhere Colmenares and Zoback (2002); Chang and Haimson (2005); Haimson (2006); Cai (2008); Walsri et al. (2009). Under true triaxial compressive stresses the modified Wiebols and Cook criterion can predict the compressive strengths of the tested sandstone reasonably well. Due to the effect of σ_2 the Coulomb criterion can not represent the rock strengths under true triaxial compressions, particularly under high σ_2 to σ_3 ratios. The mean misfit is 51.65 MPa for the Coulomb criterion and is 2.93 MPa for the modified Wiebols and Cook criterion. PW sandstone shows isotropic property with the elastic modulus and Poisson's ratio averaged as 10.31 ± 0.71 GPa and 0.26 ± 0.02. The observed variation may be due to the intrinsic variability of the rock.

It is postulated that the effects of the intermediate principal stress are caused by two mechanisms working simultaneously but having opposite effects on the rock

polyaxial strengths; (1) mechanism that strengthens the rock matrix in the direction normal to σ_1 - σ_3 plane, and (2) mechanism that induces tensile strains in the directions of σ_1 and σ_3. The intermediate principal stress can strengthen the rock matrix on the plane normal to its direction, and hence a higher differential stress is required to induce failure. Considering this effect alone, the higher the magnitude of σ_2 applied, the higher σ_1 (or $J_2^{1/2}$) is required to fail the specimen. Nevertheless it is believed that the relationship between σ_2 magnitudes and the degrees of strengthening can be non-linear, particularly under high σ_2. Such relation depends on rock types and their texture (e.g., distribution of grain sizes, pore spaces, fissures and micro-cracks, and types of rock-forming minerals).

6.2   Recommendations for future studies

The uncertainties and adequacies of the research investigation and results discussed above lead to the recommendations for further studies. The test should be performed on a variety of rock types with different strengths. Higher σ_2 and σ_3 values should be applied to asses the effect of σ_2 under a much higher confining pressure (σ_3). The effect of friction at the interface between the loading platen and rock surfaces should be investigated. Modification of the polyaxial load frame should be made to allow a much higher lateral stress on the samples. Size effect on the rock poly-axial strength should also be examined.

REFERENCES

Al-Ajmi, A.M., and Zimmerman, R.W. (2005). Relation between the Mogi and the Coulomb failure criteria. **International Journal of Rock Mechanics & Mining Sciences**. 42:431-439.

Alsayed, M.I. (2002). Utilising the hoek triaxial cell for multiaxial testing of hollow rock cylinders. **International Journal of Rock Mechanics & Mining Sciences**. 39: 355-366.

Cai, M. (2008). Influence of intermediate principal stress on rock fracturing and strength near excavation boundaries—Insight from numerical modeling. **International Journal of Rock Mechanics & Mining Sciences.** 45: 763-772.

Chang, C., and Haimson, B. (2005). Non-dilatant deformation and failure mechanism in two Long Valley Caldera rocks under true triaxial compression. **International Journal of Rock Mechanics & Mining Sciences.** 42: 402-414.

Colmenares, L.B., and Zoback, M.D. (2002). A statistical evaluation of intact rock failure criteria constrained by polyaxial test data for five different rocks. **International Journal of Rock Mechanics & Mining Sciences**. 39: 695-729.

Franklin, J.A., and Hoek, E. (1970). Developments in triaxial testing equipment. **Rock Mechanics**. 2: 223-228.

Haimson, B., and Chang, C. (2000). A new true triaxial cell for testing mechanical properties of rock, and its use to determine rock strength and deformability of Westerly granite. **International Journal of Rock Mechanics and Mining Sciences**. 37 (1-2): 285-296.

Haimson, B.C., and Chang, C. (2001). True triaxial testing of crystalline rocks reveals new mechanical properties and micromechanics of brittle fracture that go unnoticed in conventional triaxial tests. **American Geophysical Union**., pp. 235-242.

Haimson, B. (2006). True triaxial stresses and the brittle fracture of rock. **Pure and Applied Geophysics**. 163 1101-1130.

Haimson, B. (2000). A new true triaxial cell for testing mechanical properties of rock, and its use to determine rock strength and deformability of westerly granite. **International Journal of Rock Mechanics & Mining Sciences**. 37: 285-296.

Hoek, E., and Brown, E.T. (1980). Underground excavations in rock. **IMM**. London, pp. 133-136.

Jaeger, J.C., and Cook, N.G.W. (1979). **Fundamentals of Rock Mechanics (3rd. Edn.)**. Chapman & Hall, London, pp. 105-106.

Kwaśniewski, M., Takahashi, M., and Li, X. (2003). Volume changes in sandstone under true triaxial compression conditions. **ISRM 2003–Technology Roadmap for Rock Mechanics**. South African Institute of Mining and Metallurgy, pp. 683-688.

Mogi, K. (1967). Effect of the intermediate principal stress on rock failure. **J Geophys. Res.** 72:5117–31.

Mogi, K. (1970). Effect of triaxial stress system on rock failure. **Rock Mech. In Japan.** 1: 53-55.

Mogi, K. (1971). Fracture and flow of rocks under high triaxial compression. **J. Geophys. Res.** 76(5): 1255-1269.

Mogi, K. (1977). Dilatancy of rocks under general triaxial stress states with special reference to earthquake precursors. **J. Phys. Earth., 25(suppl.),** pp. S203-S217.

Rao, K.S., and Tiwari, R.P. (2002). Physical simulation of jointed model materials under biaxial and true triaxial stress states. **Research Report, IIT Delhi, India,** pp. 30.

Riley, K.F., Hobson, M.P., and Bence, S.J. (1998). **Mathematical Methods for Physics and Engineering.** Cambridge: Cambridge University Press, 1008 pp.

Singh, B., Goel, R.K., Mehrotra, V.K., Garg, S.K., and Allu, M.R. (1998). Effect of intermediate principal stress on strength of anisotropic rock mass. **Tunneling and Underground Space Technology**. 13: 71-79.

Tiwari, R.P., and Rao, K.S. (2004). Physical modeling of a rock mass under a true triaxial stress state. **International Journal of Rock Mechanics and Mining Sciences**. 41: 1-6.

Tiwari, R.P., and Rao, K.S. (2006). Post failure behaviour of a rock mass under the influence of triaxial and true triaxial confinement. **Engineering Geology**. 84: 112-129.

Walsri, C., Poonprakon, P., Thosuwan R., and Fuenkajorn, K. (2009). Compressive and tensile strengths of sandstones under true triaxial stresses. In **Proceeding 2nd Thailand Symposium on Rock Mechanics**. Chonburi, Thailand. 2: 199-218.

Wang, Q., and Lade, P.V. (2001). Shear banding in true triaxial tests and its effect on failure in sand. **J. Engrg. Mech**. 127: 754-761.

Wiebols, G.A., and Cook, N.G.W. (1968). An energy criterion for the strength of rock in polyaxial compression. **International Journal of Rock Mechanics and Mining Sciences.** 5: 529-549.

Yang, X.L., Zou, J.F., and SUI, Z.R. (2007). Effect of intermediate principal stress on rock cavity stability. **Journal Central South University Technology**. s1-0165-05.

You, M. (2008). True-triaxial strength criteria for rock. **International Journal of Rock Mechanics and Mining Sciences.** 46: 115-127.

Zhou, S. (1994). A program to model the initial shape and extent of borehole breakout. **Comput Geosci**. 20(7/8):1143–60.

APPENDIX A

LIST OF STRESS-STRAIN CURVES
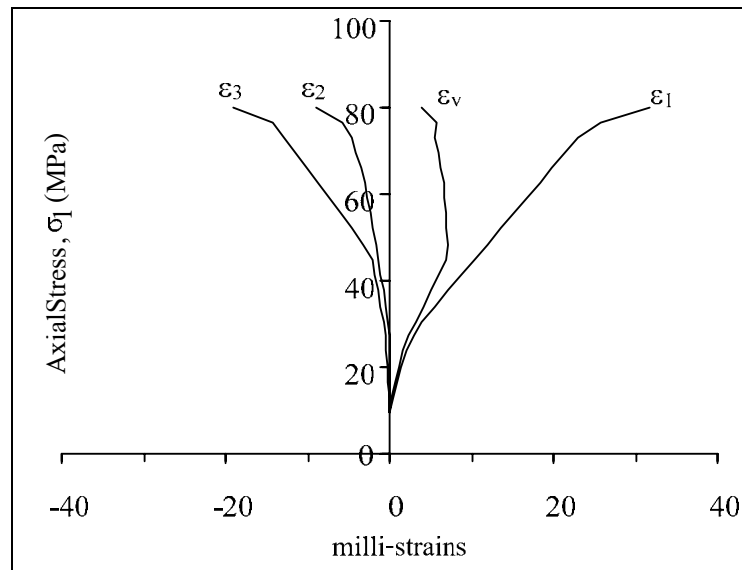
Figure A-1 Stress-strain curves of Phra Wihan sandstone tested under $\sigma_2 = 10.0$ MPa

and $\sigma_3 = 2.3$ MPa.
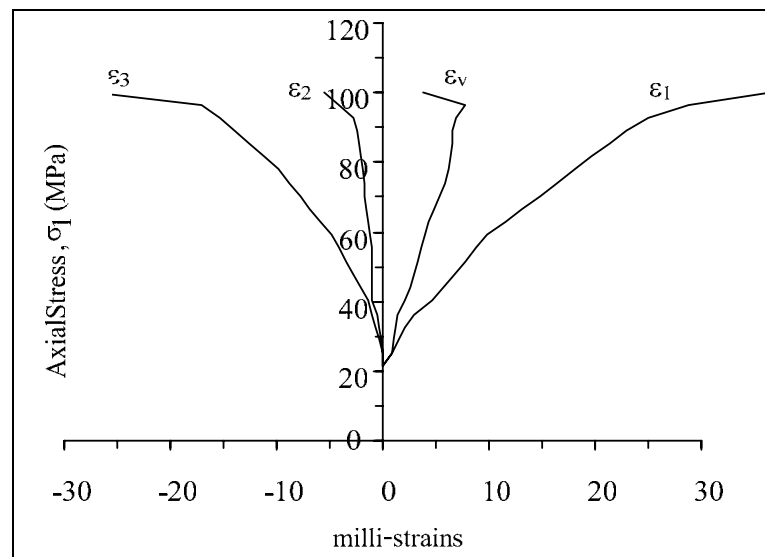
Figure A-2 Stress-strain curves of Phra Wihan sandstone tested under $\sigma_2 = 20.0$MPa
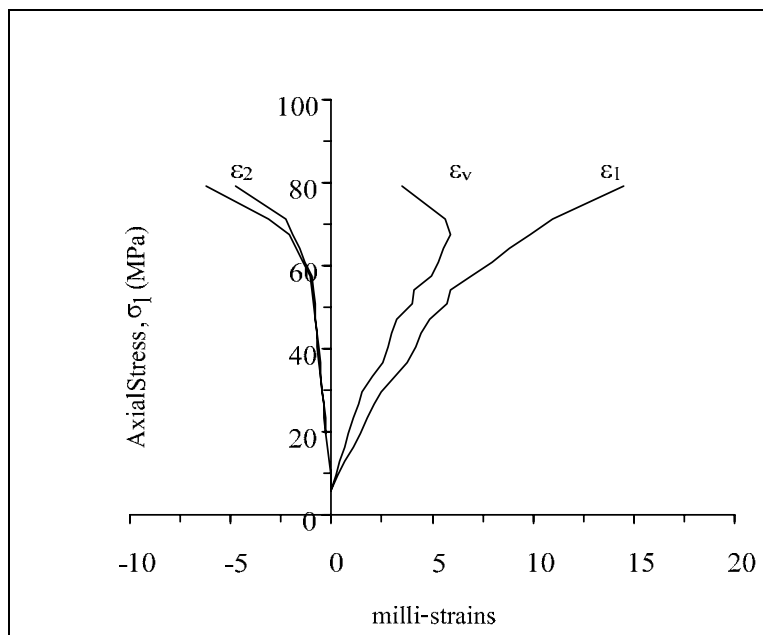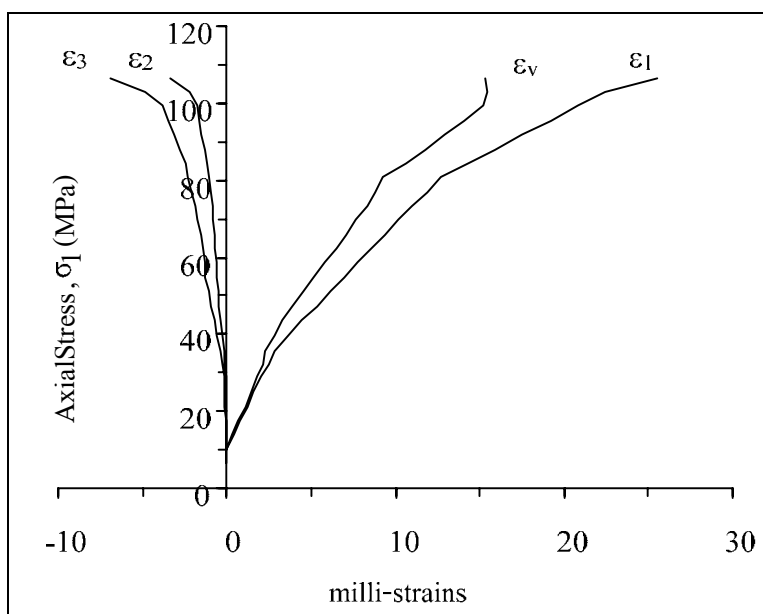
and $\sigma_3 = 2.3$ MPa.
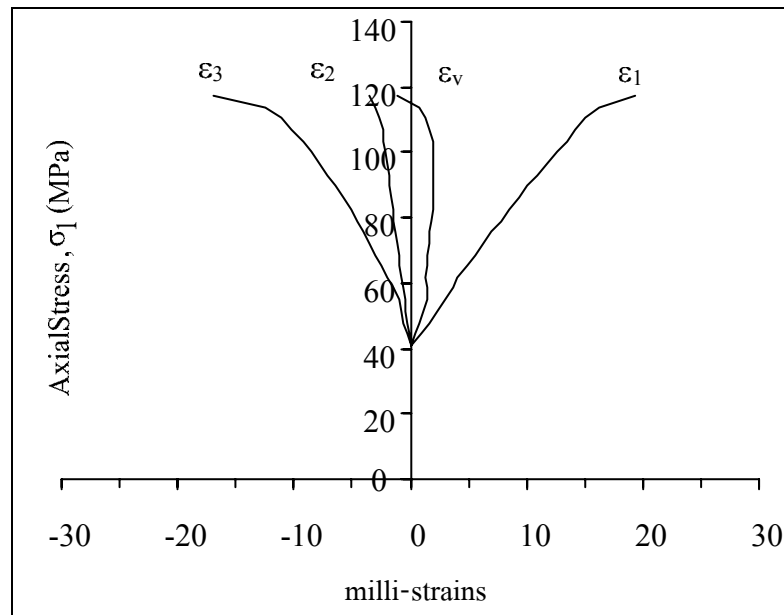
Figure A-3 Stress-strain curves of Phra Wihan sandstone tested under $\sigma_2 = 40.0$ MPa

and $\sigma_3 = 2.3$ MPa.
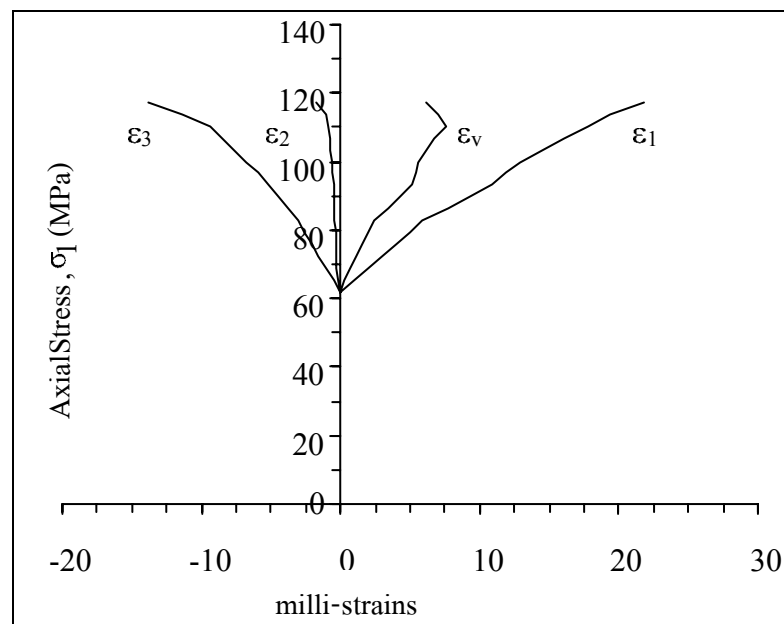
Figure A-4 Stress-strain curves of Phra Wihan sandstone tested under $\sigma_2 = 60.0$ MPa
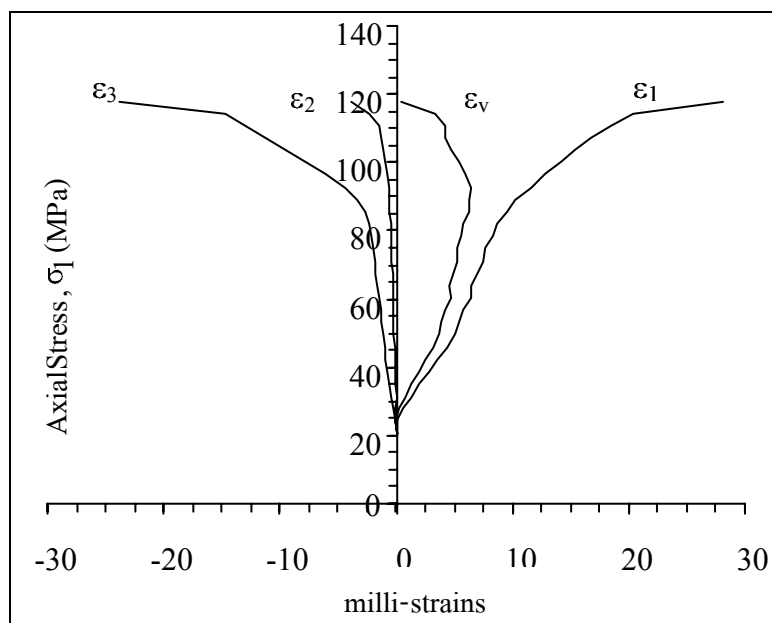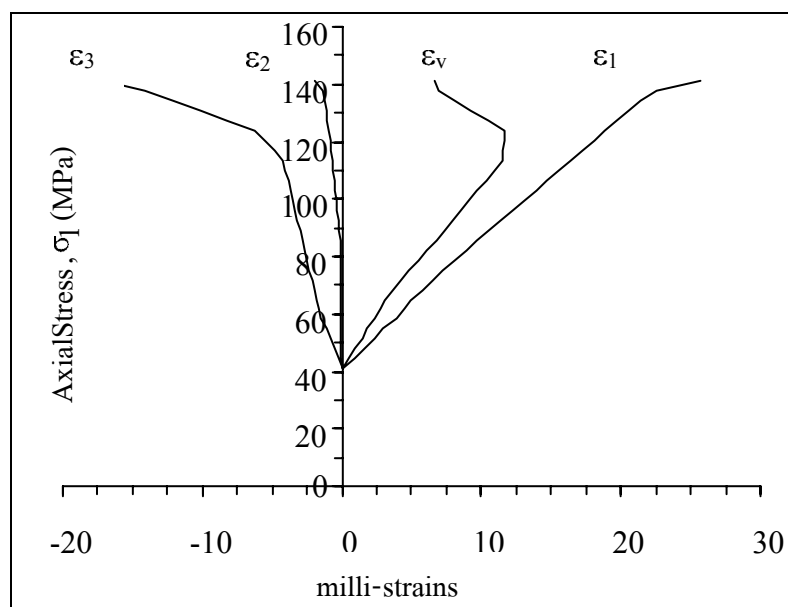
and $\sigma_3 = 2.3$ MPa.
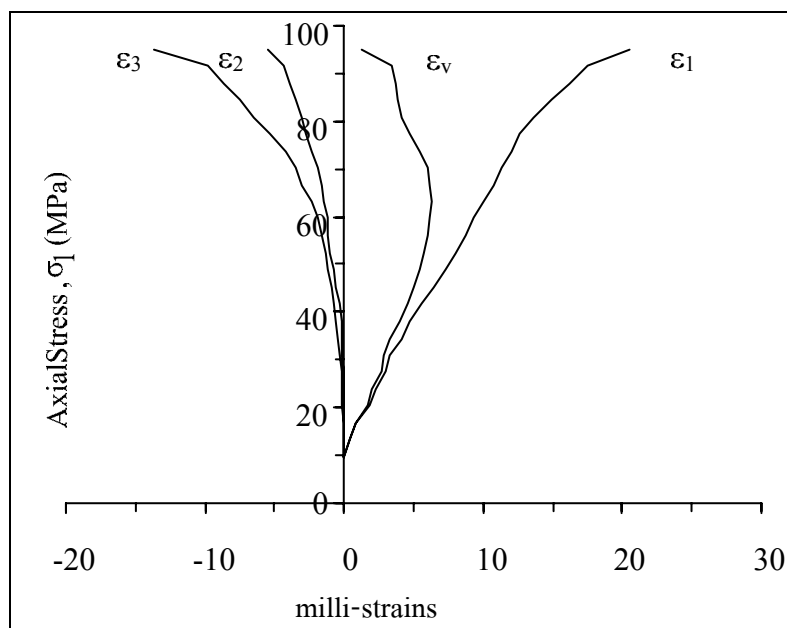
Figure A-5 Stress-strain curves of Phra Wihan sandstone tested under σ_2 = 10.0 MPa

and σ_3 = 4.1 MPa.
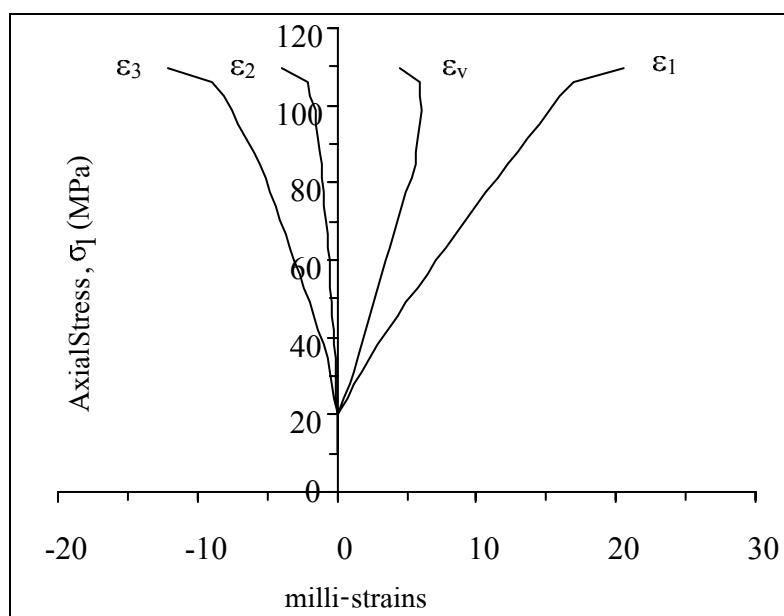
Figure A-6 Stress-strain curves of Phra Wihan sandstone tested under σ_2 = 20.0MPa

and σ_3 = 4.1 MPa
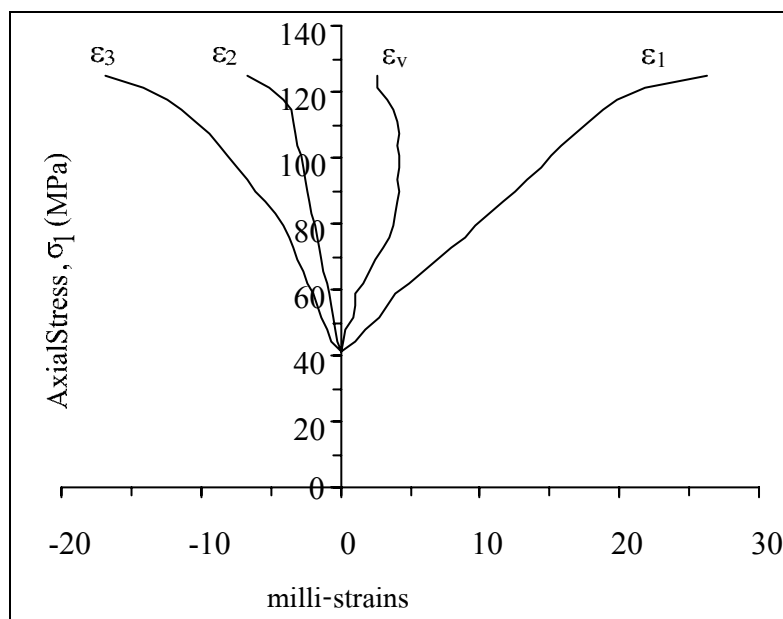
Figure A-7 Stress-strain curves of Phra Wihan sandstone tested under $\sigma_2 = 40.0$ MPa
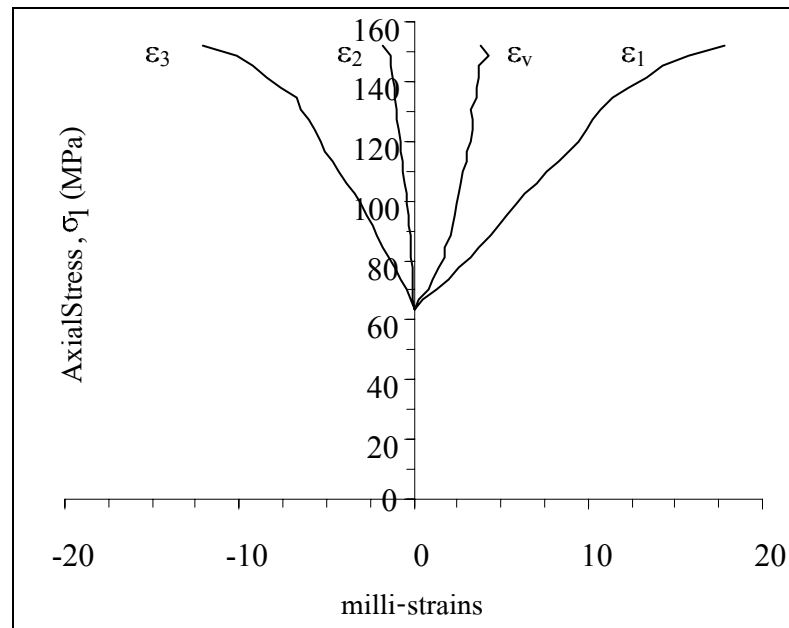
and $\sigma_3 = 4.1$ MPa.
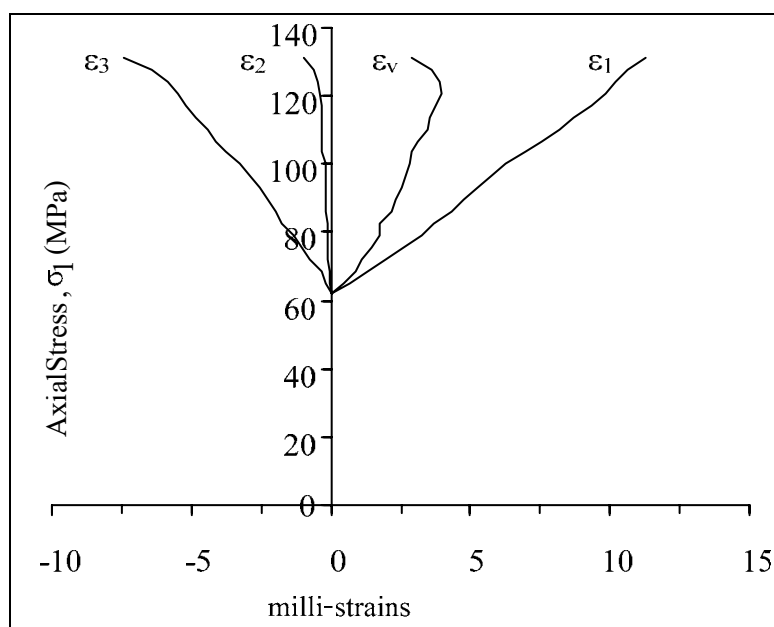
Figure A-8 Stress-strain curves of Phra Wihan sandstone tested under $\sigma_2 = 60.0$ MPa
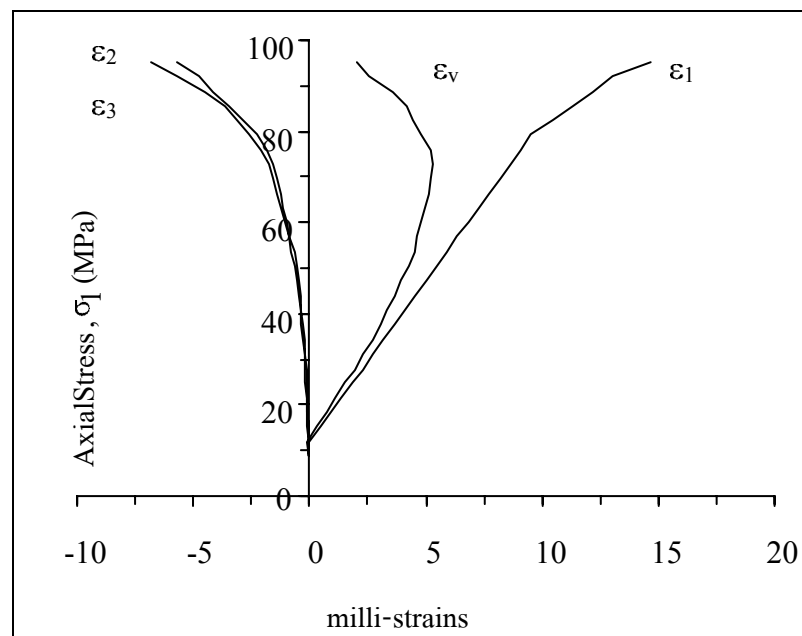
and $\sigma_3 = 4.1$ MPa.

Figure A-9 Stress-strain curves of Phra Wihan sandstone tested under σ_2 = 6.6 MPa

and σ_3 = 6.5 MPa.

Figure A-10 Stress-strain curves of Phra Wihan sandstone tested under σ_2 = 10.0 MPa

and σ_3 = 6.6 MPa.

Figure A-11 Stress-strain curves of Phra Wihan sandstone tested under $\sigma_2 = 20.0$ MPa

and $\sigma_3 = 6.6$ MPa.

Figure A-12 Stress-strain curves of Phra Wihan sandstone tested under $\sigma_2 = 40.0$ MPa

and $\sigma_3 = 6.6$ MPa.

Figure A-13 Stress-strain curves of Phra Wihan sandstone tested under $\sigma_2 = 60.0$ MPa

and $\sigma_3 = 6.6$ MPa.

Figure A-14 Stress-strain curves of Phra Wihan sandstone tested under $\sigma_2 = 8.3$ MPa
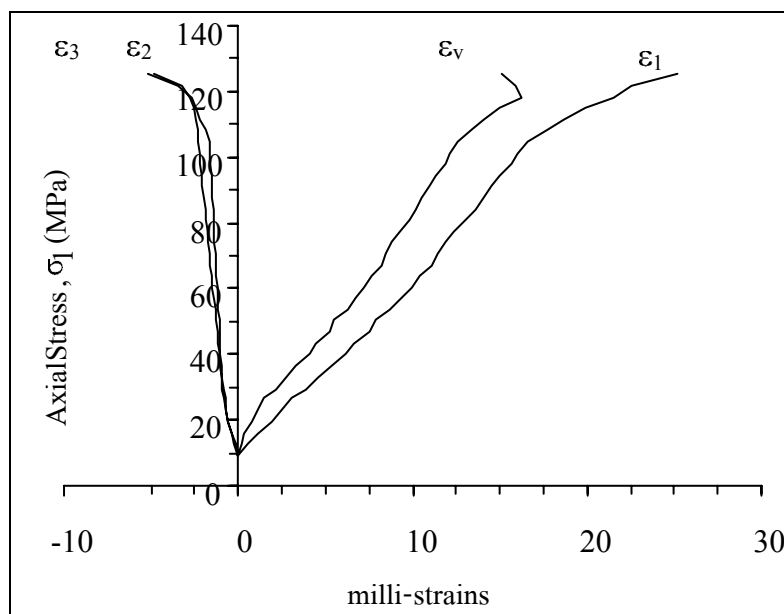
and $\sigma_3 = 8.3$ MPa.

Figure A-15 Stress-strain curves of Phra Wihan sandstone tested under $\sigma_2 = 10.1$ MPa
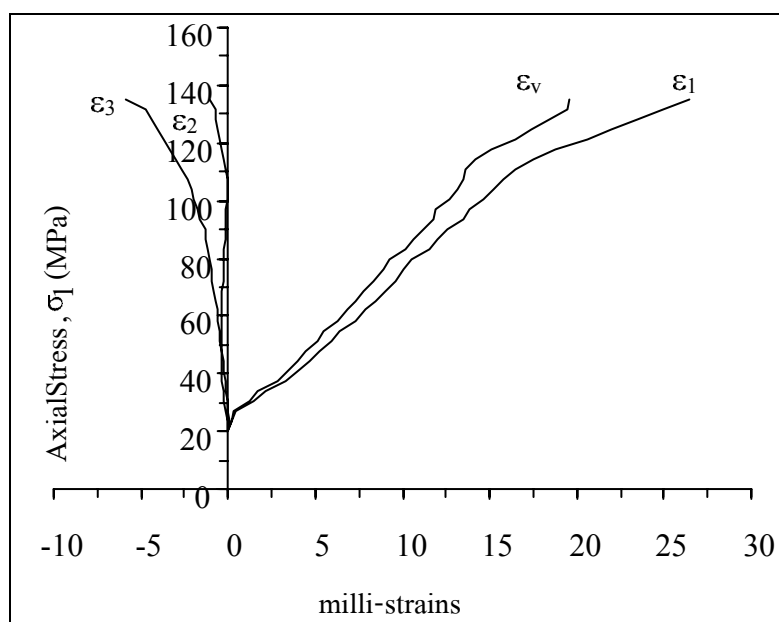
and $\sigma_3 = 10.0$ MPa.

Figure A-16 Stress-strain curves of Phra Wihan sandstone tested under $\sigma_2 = 20.0$ MPa
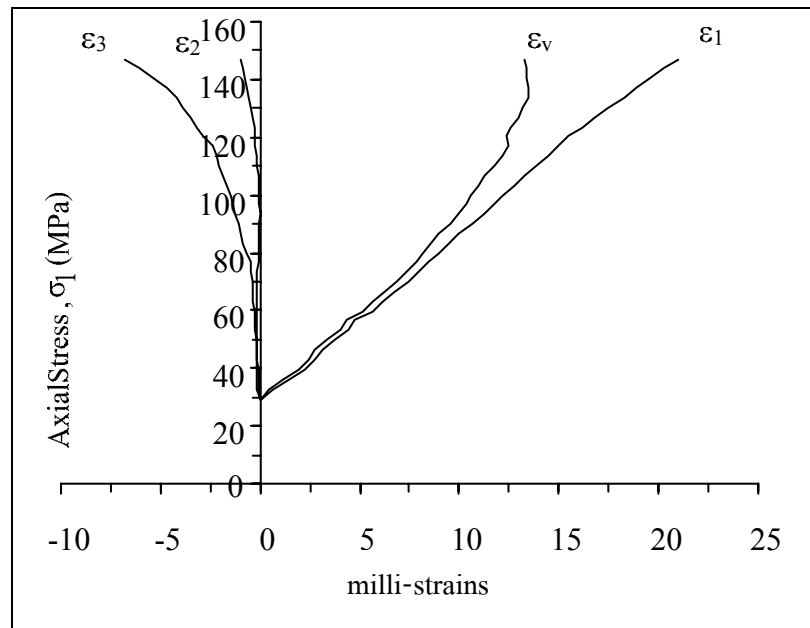
and $\sigma_3 = 10.1$ MPa.

Figure A-17 Stress-strain curves of Phra Wihan sandstone tested under $\sigma_2 = 30.0$ MPa
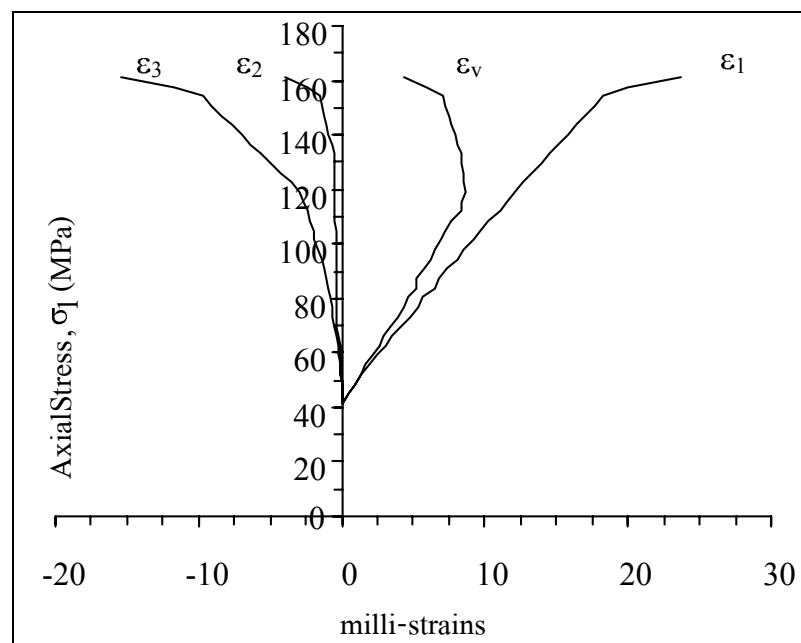
and $\sigma_3 = 10.1$ MPa.

Figure A-18 Stress-strain curves of Phra Wihan sandstone tested under $\sigma_2 = 40.0$ MPa
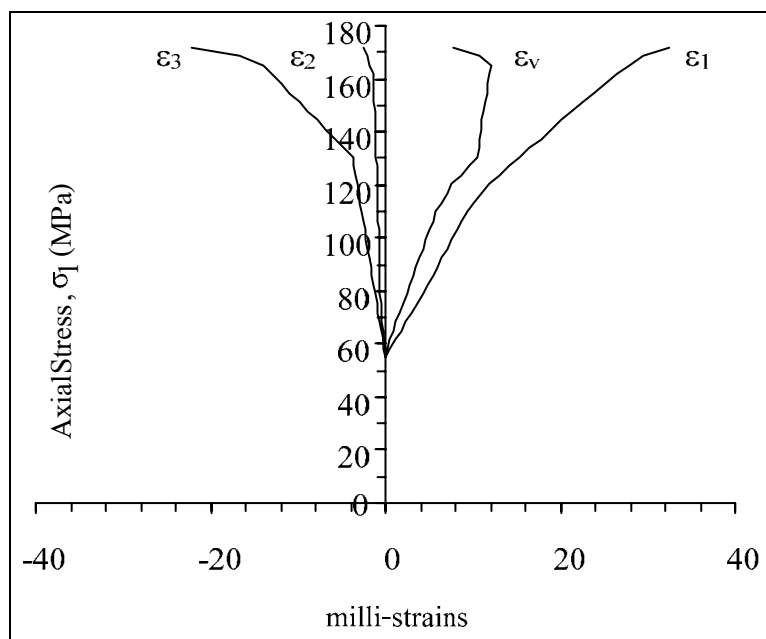
and $\sigma_3 = 10.1$ MPa.

Figure A-19 Stress-strain curves of Phra Wihan sandstone tested under $\sigma_2 = 50.0$ MPa and $\sigma_3 = 10.1$ MPa.
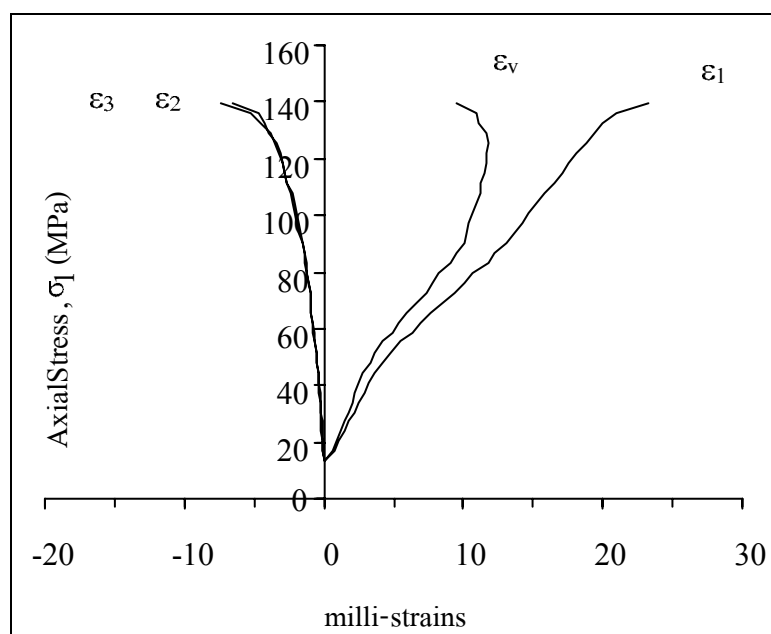

Figure A-20 Stress-strain curves of Phra Wihan sandstone tested under $\sigma_2 = 12.0$ MPa and $\sigma_3 = 12.0$ MPa.
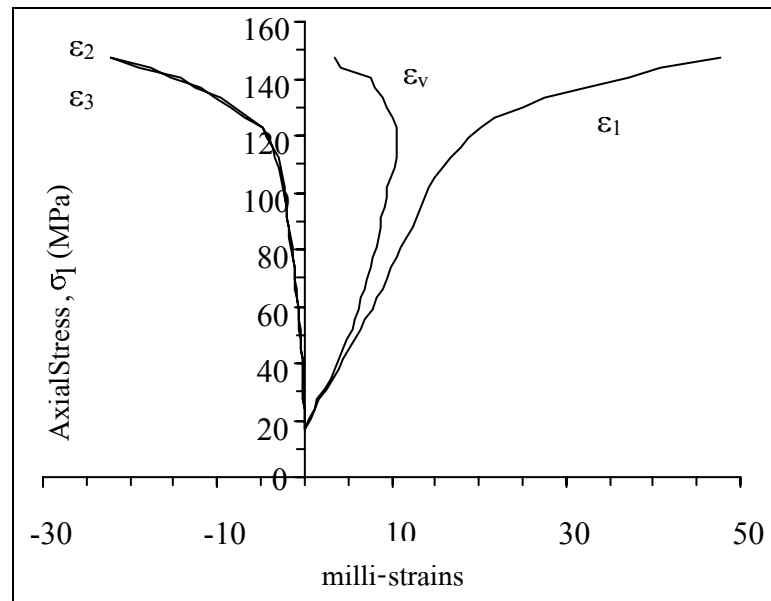
Figure A-21 Stress-strain curves of Phra Wihan sandstone tested under $\sigma_2 = 15.5$ MPa

and $\sigma_3 = 15.5$ MPa.
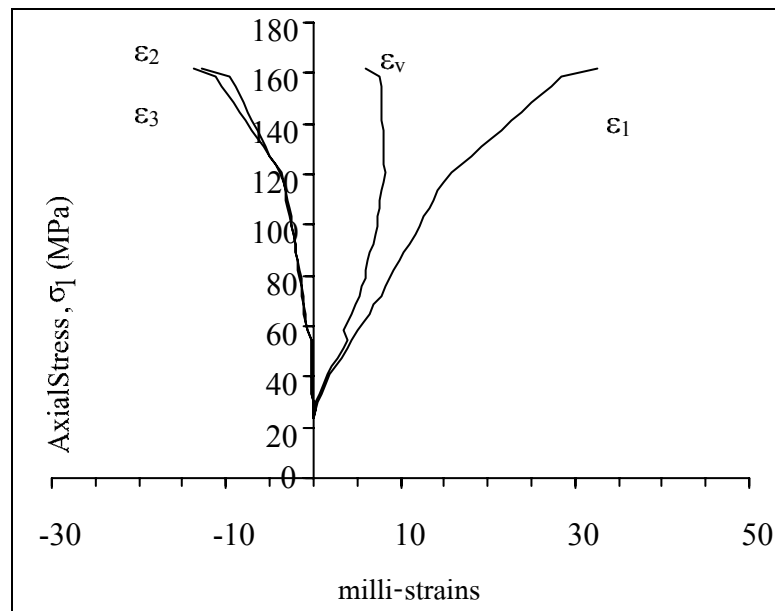
Figure A-22 Stress-strain curves of Phra Wihan sandstone tested under $\sigma_2 = 20.0$ MPa

and $\sigma_3 = 20.0$ MPa.

APPENDIX B

TECHNICAL PUBLICATION

TECHNICAL PUBLICATION

Pobwandee, T., and Fuenkajorn, K. (2011). **Effect of intermediate principal stresses on compressive strength of Phra Wihan sandstone**. The third Thailand symposium on rock mechaics. Springfield Resort & Spa, Cha-Am Beach, Thailand, 10-11 March 2011. (Accepted)

Subject: Paper Acceptance at ThaiRock 2011

Dear : Mr. Pobwandee

We are pleased to inform you that your paper, titled "Effect of intermediate principal stresses on compressive strength of Phra Wihan sandstone"by T. Pobwandee & K. Fuenkajorn, is accepted to be presented at the Third Thailand Symposium on Rock Mechanics (ThaiRock 2011). The symposium will be held on March 10-11, 2011 at the Springfield Resort & Spa, Cha-Am Beach, Thailand. Your 15-minutes oral presentation will be scheduled in a technical session at the symposium. The final technical program will be posted by early February, 2011.

Please note that you have to submit a completed registration form along with the payment before January 15th, 2011, in order to include your paper in the printed proceedings and presentation program. Please visit our website at www.geomechsut.com for instruction.

We have blocked a limited number of rooms at the Springfield Resort & Spa. If you choose to stay at the Springfield Resort, your reservation must be made by using the symposium registration form and send to us before January 15th.

Note that there are several other hotels and resorts within walking distance from the conference venue. Please check their websites for more details.

Again, thank you kindly for your participation in the Third Thailand Symposium on Rock Mechanics. We look forward to meeting you at the Cha-Am Beach soon.

Sincerely yours

Kittitep Fuenkajorn
Noppadol Phien-wej
Editors & Chairs, ThaiRock 2011

Geomechanics Research Unit
Institute of Engineering
Suranaree University of Technology
111 University Avenue, Muang District
Nakhon Ratchasima 30000 THAILAND

kittitep@sut.ac.th
fuenkajorn@yahoo.com
noppadol@ait.ac.th
gmr@sut.ac.th

Tel: 66 44-224-443
Fax: 66 44 224-448

Effect of intermediate principal stresses on compressive strength of Phra Wihan sandstone

T. Pobwandee & K. Fuenkajorn
Geomechanics Research Unit, Suranaree University of Technology, Thailand

Keywords: True triaxial, intermediate principal stress, sandstone

ABSTRACT: A polyaxial load frame has been used to determine the compressive strength of Phra Wihan sandstone under true triaxial stresses. The rock specimens are cubic shape with a nominal dimension of $5\times5\times5$ cm^3. Under a low σ_3, σ_1 at failure initially increases with σ_2 and then decreases with σ_2. Under a high σ_3, σ_1 increases with σ_2. The Coulomb and modified Wiebols & Cook failure criteria derived from the characterization test results predict the sandstone strengths in terms of $J_2^{1/2}$ as a function of J_1 under true triaxial stresses. The modified Wiebols & Cook criterion describes the failure stresses better than does the Coulomb criterion.

1 INTRODUCTION

The effects of confining pressures at great depths on the mechanical properties of rocks are commonly simulated in a laboratory by performing triaxial compression testing of cylindrical rock core specimens. A significant limitation of these conventional methods is that the intermediate and minimum principal stresses are equal during the test while the actual in-situ rock is normally subjected to an anisotropic stress state where the maximum, intermediate and minimum principal stresses are different ($\sigma_1 \neq \sigma_2 \neq \sigma_3$). It has been commonly found that compressive strengths obtained from conventional triaxial testing can not represent the actual in-situ strength where the rock is subjected to an anisotropic stress state (Yang et al. (2007), Haimson (2006), Tiwari & Rao (2006), Tiwari & Rao (2004) and Haimson & Chang (1999)).

From the experimental results on brittle rocks obtained from Colmenares & Zoback (2002) and Haimson (2006) it can be generally concluded that in a σ_1 - σ_2 diagram, for a given σ_3, σ_1 at failure initially increases with σ_2 to a certain magnitude, and then it gradually decreases as σ_2 increases. The effect of σ_2 is more pronounced under higher σ_3. The effect of σ_2 is related to the stress-induced anisotropic properties and behavior of the rock and to the end effect at the interface between the rock surface and loading platen in the direction of σ_2 application. The effect is smaller in homogeneous and fine-grained rocks than in coarse-grained rocks where pre-existing micro-cracks are not uniformly distributed.

Several failure criteria have been developed to describe the rock strength under true triaxial stress states. Comprehensive reviews of these criteria have been given recently by

1

Colmenares & Zoback (2002), Al-Ajmi & Zimmerman (2005) and Haimson (2006). Among several other criteria, the Mogi and modified Wiebols & Cook criteria are perhaps the most widely used to describe the rock compressive strengths under true triaxial stresses. Obtaining rock strengths under an anisotropic stress state is not only difficult but also expensive. A special loading device (e.g. polyaxial loading machine or true triaxial load cell) is required. As a result test data under true triaxial stress conditions have been relatively limited. Most researchers above have used the same sets of test data (some obtained over a decade ago) to compare with their new numerical simulations or field observations (notably on breakout of deep boreholes) and to verify their new strength criteria and concepts. Due to the cost and equipment availability for obtaining true triaxial strengths, in common engineering practices application of a failure criterion that can incorporate the three-dimensional stresses has been very rare used.

The objective of this study is to determine the effects of the minimum principal stress on the compressive strength of Phra Wihan sandstones. The Coulomb and modified Wiebols & Cook failure criteria derived from the results of conventional tests are used to describe the compressive strengths of the rocks under true triaxial stress states. Assessment of the predictive capability of the two criteria is also made.

2 ROCK SAMPLES

The tested sandstone is from Phra Wihan formation (PW sandstone). It is fine-grained quartz sandstone. It is selected primarily because of its highly uniform texture, density and strength. Its average grain size is 0.1-1.0 mm. The rock is commonly found in the north and northeast of Thailand. Its mechanical properties and responses play a significant role in the stability of tunnels, slope embankments and dam foundations in the region. For the polyaxial compression testing cubical block specimens are cut and ground to have a nominal dimension of $5\times5\times5$ cm^3.

3 POLYAXIAL COMPRESSION TESTS

A polyaxial load frame equipped with a cantilever beam system (Walsri et al., 2009) has been used to apply constant and uniform lateral stresses (confining pressures) to the cubical specimen while the axial stress is increased at a constant rate until failure occurs (Figure 1). The compression tests are performed to determine the compressive strengths and deformations of the PW sandstone under true triaxial stresses. The intermediate (σ_2) and minimum (σ_3) principal stresses are maintained constant while σ_1 is increased until failure occurs. In this study, σ_2 is varied from 6.6 to 60 MPa, and σ_3 from 2.3 to 15 MPa. Neoprene sheets are used to minimize the friction at all interfaces between the loading platen and the rock surface.

Figure 2 plots the stress-strain curve from the start of loading to failure for some specimens. The elastic modulus and Poisson's ratio are calculated. The three-dimensional principal stress-strain relations given by Jaeger & Cook (1979) can be simplified to obtain a set of governing equations for a isotropic material as follows:

$$\varepsilon_1 = \frac{\sigma_1}{E} - \frac{\nu}{E}(\sigma_2 + \sigma_3) \tag{1}$$
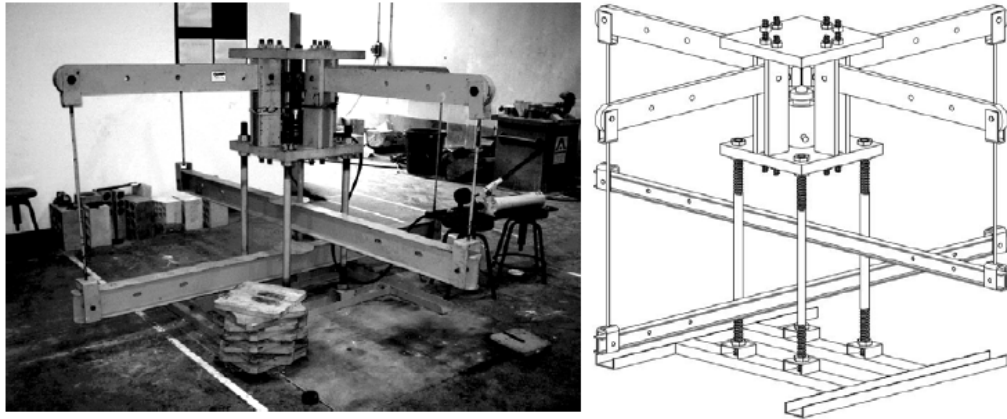
2

Figure 1. Polyaxial load frame developed for compressive strength testing under true triaxial stresses.
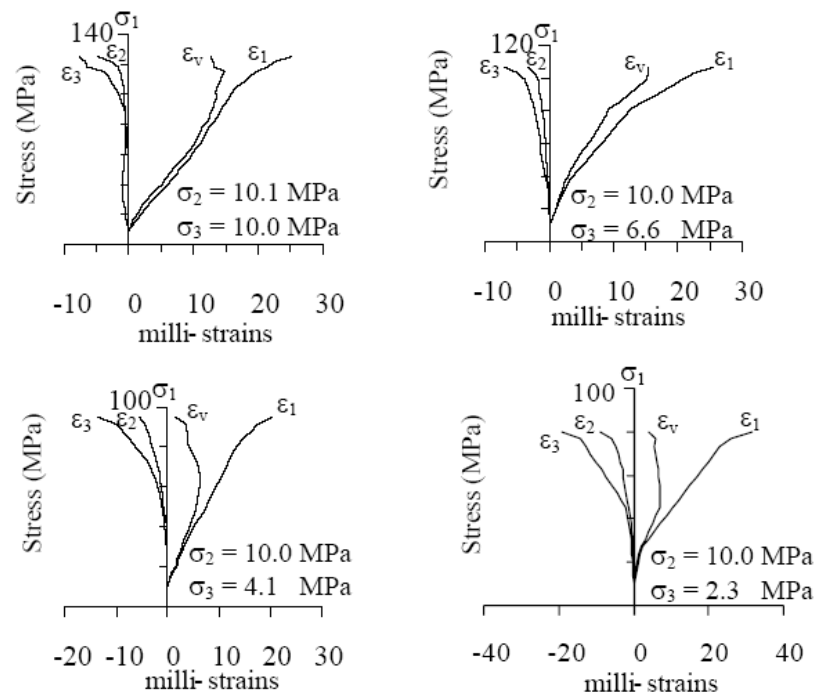

Figure 2. Examples of stress-strain curves obtained from polyaxial compressive strength test.

$$\varepsilon_2 = \frac{\sigma_2}{E} - \frac{\nu}{E}(\sigma_1 + \sigma_3) \qquad (2)$$

$$\varepsilon_3 = \frac{\sigma_3}{E} - \frac{\nu}{E}(\sigma_1 + \sigma_2) \qquad (3)$$

where σ_1, σ_2 and σ_3 are principal stresses, ε_1, ε_2 and ε_3 are principal strains, E is elastic modulus, and ν is Poisson's ratio.

The calculations of the Poisson's ratios and tangent elastic moduli are made at 50% of the maximum principal stress. Table 1 summarizes the results for each sample.

Figure 3 plots σ_1 at failure as a function of σ_2 tested under various σ_3's for PW sandstone. The results show the effects of the intermediate principal stress, σ_2, on the maximum stresses at failure by the failure envelopes being offset from the condition where $\sigma_2=\sigma_3$. For all minimum principal stress levels, σ_1 at failure increases with σ_2. The effect of σ_2 tends to be more pronounced under a greater σ_3. These observations agree with those obtained elsewhere (e.g. Haimson & Chang (1999), Colmenares & Zoback (2002) and Haimson (2006)). Post-failure observations suggest that compressive shear failures are predominant in the specimens tested under low σ_2 while splitting tensile fractures parallel to σ_1 and σ_2 directions dominate under higher σ_2 (Figure 4). The observed splitting tensile fractures under relatively high σ_2 suggest that the fracture initiation has no influence from the friction at the loading interface in the σ_2 direction. As a result the increase of σ_1 with σ_2 should not be due to the interface friction.

Table 1. Summary of the polyaxial compressive strength test results on PW sandstone.

Specimen No.	σ_3 (MPa)	σ_2 (MPa)	σ_1 (MPa)	E (GPa)	ν
PWSS-PX-38	2.3	10.0	80.3	9.87	0.28
PWSS-PX-03		20.0	100.3	10.75	0.25
PWSS-PX-58		40.0	117.4	10.89	0.25
PWSS-PX-55		60.0	117.4	10.74	0.28
PWSS-PX-44	4.1	10.0	95.0	10.62	0.23
PWSS-PX-08		20.0	109.5	9.87	0.28
PWSS-PX-27		40.0	124.8	11.88	0.25
PWSS-PX-01		60.0	131.2	10.74	0.27
PWSS-PX-42	6.5	6.6	94.5	9.19	0.27
PWSS-PX-30	6.6	10.0	106.6	10.78	0.25
PWSS-PX-33		20.0	118.0	11.14	0.28
PWSS-PX-45		40.0	141.1	10.92	0.28
PWSS-PX-02		60.0	150.2	10.72	0.27
PWSS-PX-21	8.3	8.3	108.9	9.31	0.26
PWSS-PX-23	10.0	10.1	125.1	9.67	0.28
PWSS-PX-34	10.1	20.0	135.0	10.49	0.24
PWSS-PX-35		30.0	147.1	9.60	0.24
PWSS-PX-32		40.0	161.2	9.24	0.27
PWSS-PX-49		50.0	172.0	10.72	0.27
PWSS-PX-29	12.0	12.0	139.2	9.83	0.28
PWSS-PX-37	15.5	15.5	147.4	10.33	0.26
PWSS-PX-46	20.0	20.0	161.9	9.55	0.28
Mean ± SD.				10.31 ± 0.71	0.26 ± 0.02
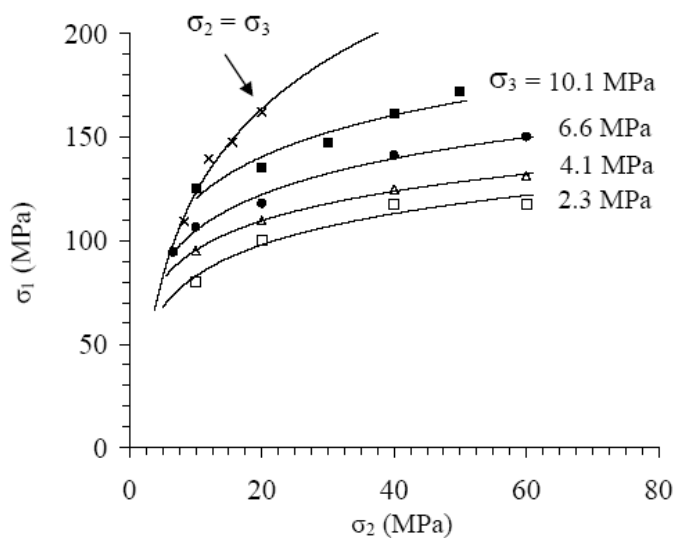
Figure 3. Maximum principal stress (σ_1) at failure as a function of σ_2 for various σ_3 values.

[80.3, 10.0, 2.3] [100.3, 20.0, 2.3] [117.4, 40.0, 2.3] [117.4, 60.0, 2.3]

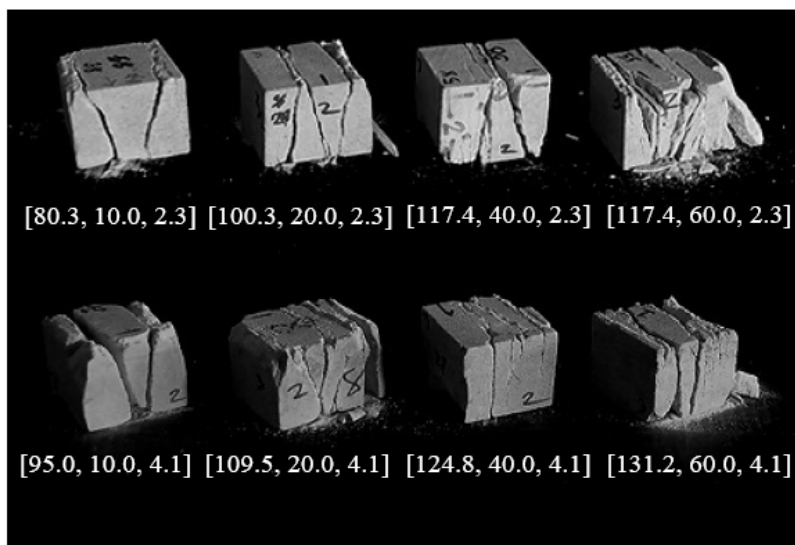[95.0, 10.0, 4.1] [109.5, 20.0, 4.1] [124.8, 40.0, 4.1] [131.2, 60.0, 4.1]

Figure 4. Some post-test specimens of PW sandstone. Number in blankets indicate [$\sigma_1,\sigma_2,\sigma_3$] at failure

4 STRENGTH CRITERIA

The Coulomb and modified Wiebols & Cook failure criteria are used to describe the polyaxial strengths of the PW sandstone. They are selected because the Coulomb criterion has been widely used in actual field applications while the modified Wiebols & Cook criterion has been claimed by many researchers to be one of the best representations of rock strengths under polyaxial compression. To represent the rock strengths under true triaxial stresses the second order stress invariant ($J_2^{1/2}$) and the first order stress invariant or the mean stress (J_1) are calculated from the test results by the following relations (Jaeger & Cook, 1979):

5

$$J_2^{1/2} = \sqrt{(1/6)\{(\sigma_1-\sigma_2)^2 + (\sigma_1-\sigma_3)^2 + (\sigma_2-\sigma_3)^2\}} \tag{4}$$

$$J_1 = (\sigma_1 + \sigma_2 + \sigma_3)/3 \tag{5}$$

In this study, the Coulomb criterion is derived from the triaxial compressive strengths of the rocks where σ_2 and σ_3 are equal. The friction angle is 48.8°, and the cohesion is 8.8 MPa. Figure 5 compares the polyaxial test results with those predicted by the Coulomb criterion for PW sandstones. The predictions are made for σ_3=2.3, 4.1, 6.6, 8.3, 10.1, 12.0, 15.5 and 20.0 MPa. (as used in the tests) and under stress conditions from $\sigma_2=\sigma_3$. In the $J_2^{1/2}$ - J_1 diagram, $J_2^{1/2}$ increases with σ_3 but it is independent of J_1 because the Coulomb criterion ignores σ_2 in the strength calculation. Under a low σ_2 and σ_3 the Coulomb prediction tends to agree with the test results obtained from the PW sandstone. Except for this case, no correlation between the Coulomb predictions and the polyaxial strengths can be found. The inadequacy of the predictability of Coulomb criterion under polyaxial stress states obtained here agrees with a conclusion drawn by Colmenares & Zoback (2002).

The modified Wiebols & Cook criterion given by Colmenares & Zoback (2002) defines $J_2^{1/2}$ at failure in terms of J_1 as:

$$J_2^{1/2} = A + BJ_1 + CJ_1^2 \tag{6}$$

The constants A, B and C depend on rock materials and the minimum principal stresses (σ_3). They can be determined under the conditions where $\sigma_2 = \sigma_3$, as follows (Colmenares & Zoback, 2002):
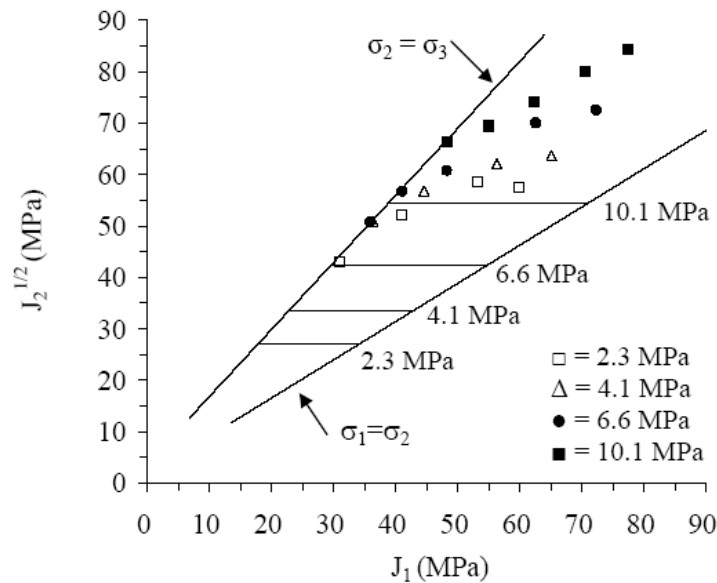

Figure 5. $J_2^{1/2}$ as a function of J_1 from testing PW sandstone compared with the Coulomb criterion predictions (lines).

6

$$C = \frac{\sqrt{27}}{2C_1 + (q-1)\sigma_3 - C_0} \times \left(\frac{C_1 + (q-1)\sigma_3 - C_0}{2C_1 + (2q+1)\sigma_3 - C_0} - \frac{q-1}{q+2} \right) \tag{7}$$

where: $C_1 = (1 + 0.6\mu_i)C_0$

$C_0 =$ uniaxial compressive strength of the rock.

$\mu_i = \tan\phi$

$q = \{(\mu_i^2 + 1)^{1/2} + \mu_i\}^2 = \tan^2(\pi/4 + \phi/2)$

$$B = \frac{\sqrt{3}(q-1)}{q+2} - \frac{C}{3}(2C_0 + (q+2)\sigma_3) \tag{8}$$

$$A = \frac{C_0}{\sqrt{3}} - \frac{C_0}{3}B - \frac{C_0^2}{9}C \tag{9}$$

The numerical values of A, B and C for PW sandstones are given in Table 2 for each σ_3 tested. Substituting these constants into equation (6), the upper and lower limits of $J_2^{1/2}$ for each rock type can be defined under conditions of $\sigma_2 = \sigma_3$ and $\sigma_1 = \sigma_2$. The predictions are made for $\sigma_3 = 2.3$, 4.1, 6.6, 8.3, 10.1, 12.0, 15.5 and 20.0 MPa. Figure 6 compares the test results with those predicted by the modified Wiebols & Cook criterion. The predictions agree well with the test results. This conforms to the results obtained by Colmenares & Zoback (2002). The predictive capability of the modified Wiebols & Cook criterion can be improved as the minimum principal stress increases.

5 CONCLUSIONS

True triaxial compressive strengths of PW sandstone have been determined in this study. Cubical specimens with a nominal dimension of 5×5×5 cm^3 are prepared. A polyaxial load frame equipped with cantilever beam is used to apply constant σ_2 and σ_3 while σ_1 (along the long axis) is increased until failure is induced. The strength results clearly show that σ_2 affects the maximum stress, σ_1 at failure for PW sandstone. Under true triaxial compressive stresses the modified Wiebols and Cook criterion can predict the compressive strengths of the tested sandstones reasonably well. Due to the effect of σ_2 the Coulomb criterion can not represent the rock strengths under true triaxial compressions, particularly under high σ_2 to σ_3 ratios. The mean misfit is 51.65 for the Coulomb criterion and is 2.93 for the modified Wiebols & Cook criterion.

Table 2. Modified Wiebols and Cook parameters for PW sandstone.

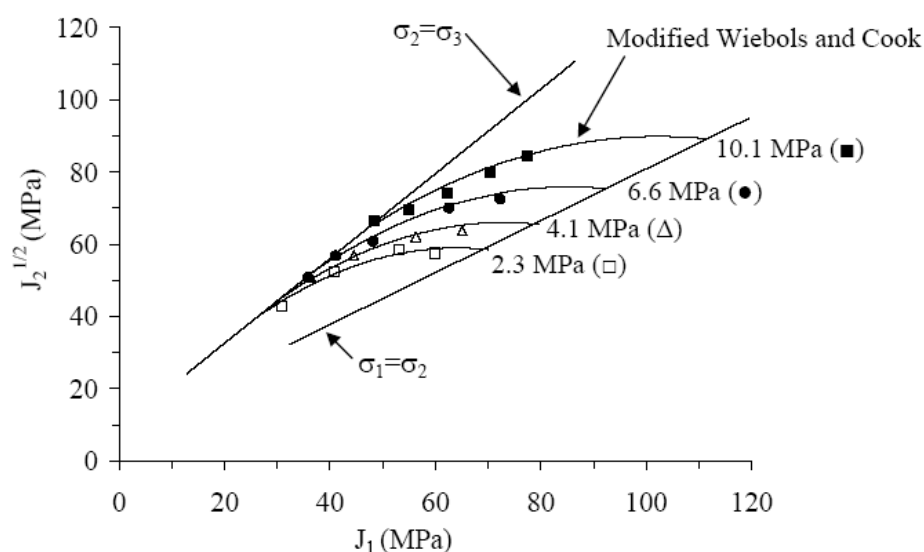| σ_3 (MPa)	Properties		
	A (MPa)	B	C (MPa^{-1})
2.3	4.311	1.706	-0.013
4.1	3.910	1.701	-0.012
6.6	3.486	1.697	-0.010
10.1	3.053	1.694	-0.008

Figure 6. $J_2^{1/2}$ as a function of J_1 from testing PW sandstone compared with the modified Wiebols & Cook criterion predictions (lines).

ACKNOWLEDGTMENT

REFERENCRS

Al-Ajmi, A.M. & Zimmerman, R.W., 2005. Relation between the Mogi and the Coulomb failure criteria. *International Journal of Rock Mechanics & Mining Sciences.* 42: 431-439.

Colmenares, L.B. & Zoback, M.D., 2002. A statistical evaluation of intact rock failure criteria constrained by polyaxial test data for five different rocks. *International Journal of Rock Mechanics & Mining Sciences.* 39: 695-729.

Haimson, B. & Chang, C., 1999. A new true triaxial cell for testing mechanical properties of rock, and its use to determine rock strength and deformability of Westerly granite. *International Journal of Rock Mechanics and Mining Sciences.* 37: 285-296.

Haimson, B., 2006. True triaxial stresses and the brittle fracture of rock. *Pure and Applied Geophysics.* 163: 1101-1113.

Jaeger, J.C. & Cook, N.G.W., 1979. *Fundamentals of Rock Mechanics.* London: Chapman and Hall.

Tiwari, R.P. & Rao, K.S., 2004. Physical modeling of a rock mass under a true triaxial stress state. *International Journal of Rock Mechanics and Mining Sciences.* 41(30).

Tiwari, R.P. & Rao, K.S., 2006. Post failure behaviour of a rock mass under the influence of triaxial and true triaxial confinement. *Engineering Geology.* 84: 112-129.

Walsri, C., Poonprakon, P., Thosuwan, R. & Fuenkajorn K., 2009. Compressive and tensile strengths of sandstones under true triaxial stresses. *Proceedings of the Second Thailand Rock Mechanics Symposium.* Nakhon Ratchasima: Suranaree University of Technology.

Yang, X. L., Zou, J. F. & SUI, Z. R., 2007. Effect of intermediate principal stress on rock cavity stability. *Journal Central South University Technology.* s1-0165-05.

BIOGRAPHY

Mr. Thanawat Pobwandee was born on March 8, 1987 in Yasothon province, Thailand. He received his Bachelor's degree in Engineering (Geotechnology) from Suranaree University of Technology in 2008. For his post-graduate, he continued to study with Master's degree in the Geological Engineering Program, Institute of Engineering, Suranaree University of Technology. During graduation, 2008-2010, he was a part time worker in position of research assistant at the Geomechanics Resaerch Unit, Institute of Engineering, Suranaree University of Technology.